

1-1-2009

Small Signal And Transient Stability Analysis Of Mvdc Shipboard Power System

Seetharama Raju Rudraraju

Follow this and additional works at: <https://scholarsjunction.msstate.edu/td>

Recommended Citation

Rudraraju, Seetharama Raju, "Small Signal And Transient Stability Analysis Of Mvdc Shipboard Power System" (2009). *Theses and Dissertations*. 3965.
<https://scholarsjunction.msstate.edu/td/3965>

This Graduate Thesis - Open Access is brought to you for free and open access by the Theses and Dissertations at Scholars Junction. It has been accepted for inclusion in Theses and Dissertations by an authorized administrator of Scholars Junction. For more information, please contact scholcomm@msstate.libanswers.com.

SMALL SIGNAL AND TRANSIENT STABILITY ANALYSIS OF MVDC
SHIPBOARD POWER SYSTEM

By

Seetharama Raju Rudraraju

A Thesis
Submitted to the Faculty of
Mississippi State University
in Partial Fulfillment of the Requirements
for the Degree of Master of Science
in Electrical Engineering
in the Department of Electrical and Computer Engineering

Mississippi State, Mississippi

December 2009

Copyright 2009

By

Seetharama Raju Rudraraju

SMALL SIGNAL AND TRANSIENT STABILITY ANALYSIS OF MVDC
SHIPBOARD POWER SYSTEM

By

Seetharama Raju Rudraraju

Approved:

Noel N. Schulz
Professor of Electrical and
Computer Engineering
(Director of Thesis)

Anurag K. Srivastava
Assistant Research Professor of Electrical
and Computer Engineering
(Co-Advisor)

Suresh C. Srivastava
Adjunct Professor of Electrical and
Computer Engineering
(Committee Member)

James E. Fowler
Professor and Director of Graduate
Studies, Electrical and Computer
Engineering

Sarah A. Rajala
Dean of Bagley College of Engineering

Name: Seetharama Raju Rudraraju

Date of Degree: December 11, 2009

Institution: Mississippi State University

Major Field: Electrical Engineering

Major Professor: Dr. Noel N Schulz

Title of Study: SMALL SIGNAL AND TRANSIENT STABILITY ANALYSIS OF
MVDC SHIPBOARD POWER SYSTEM

Pages in Study: 84

Candidate for Degree of Master of Science

Recent developments in high power rated Voltage Source Converters (VSCs) have resulted in their successful application in Multi-Terminal HVDC (MTDC) transmission systems and also have potential in the Medium Voltage DC (MVDC) distribution systems. This work presents the findings of stability studies carried out on a zonal MVDC architecture for the shipboard power distribution system. The stability study is confined to rotor angle stability of the power system, i.e. the transient and small signal stability analysis. The MTDC ring structure similar to MVDC shipboard power system was implemented in MATLAB/Simulink to look at the transient behavior of the MVDC system. Small signal stability analysis has been carried out with the help of Power System Toolbox (PST) for both MVAC as well as MVDC architectures. Later, Participation Analysis has been carried out to address the small signal instability in the case of MVAC architecture and methods for enhancement were also presented.

DEDICATION

I would like to dedicate this thesis to my parents and grandfather.

ACKNOWLEDGEMENTS

I would like to thank Dr. Noel N Schulz, my advisor, for her guidance, motivation, constant encouragement and financial support. I am happy for working and being a part of the Power and Energy Research Lab (PERL) at Mississippi State.

I am thankful to Dr. Anurag K Srivastava, my co-advisor, for his suggestions and support throughout my work.

Special thanks to Dr. Suresh C Srivastava for guiding me throughout the research work. His vast technical knowledge and experience helped me greatly in solving many problems encountered during my research work.

I would like to thank Office of Naval Research (ONR) for the financial support during my Master's degree.

Last but not least, I would like to thank my friends and colleagues at MSU for their help and support.

TABLE OF CONTENTS

	Page
DEDICATIONii
ACKNOWLEDGEMENTSiii
LIST OF TABLESvii
LIST OF FIGURESviii
LIST OF ACRONYMSx
CHAPTER	
1. INTRODUCTION	1
1.1 Introduction	1
1.2 Shipboard Power System Architectures	1
1.3 Stability Studies.....	2
1.4 Objective of Thesis.....	3
1.5 Thesis Outline.....	4
2. BACKGROUND AND LITERATURE REVIEW	5
2.1 Introduction	5
2.2 Zonal Shipboard Power System Architectures.....	7
2.2.1 MVAC architecture:.....	7
2.2.2 MVDC Architecture.....	8
2.3 Literature Review on VSC based HVDC.....	10
2.4 Voltage Source Converter	11
2.4.1 Two level VSC.....	15
2.4.2 Three level VSC.....	16
2.5 VSC-HVDC System.....	17
2.5.1 Converters	18
2.5.2 Converter Transformers	18
2.5.3 AC Filters.....	18
2.5.4 Phase Reactors	19
2.5.5 DC Capacitors.....	19
2.5.6 DC Cables	20
2.6 Concept of Multi-Terminal DC	21

2.7	Advantages and Applications of VSC-HVDC	23
2.8	Summary.....	24
3.	PROBLEM STATEMENT AND DESCRIPTION	25
3.1	Introduction	25
3.2	Problem Statement.....	25
3.3	Classification of Stability Problem.....	26
3.3.1	Rotor Angle Stability	27
3.3.2	Frequency Stability	29
3.3.3	Voltage Stability	29
3.4	Problem Description.....	30
3.4.1	Transient Stability.....	30
3.4.2	Small signal stability.....	31
3.5	Summary.....	33
4.	MODELING AND TRANSIENT STABILITY ANALYSIS OF VSC- MVDC SYSTEMS.....	34
4.1	Introduction	34
4.2	Control of VSC.....	34
4.2.1	Constant DC Voltage Regulator	37
4.2.2	Constant Power Regulator	39
4.3	Tuning of PI Controllers.....	41
4.3.1	Modulus Optimum Condition.....	41
4.3.2	Symmetrical Optimum Condition.....	42
4.4	Two-Terminal VSC-MVDC.....	43
4.5	Multi-Terminal DC Ring Structure	46
4.6	Transient Stability Analysis for MTDC Ring Structure.....	49
4.7	Summary.....	50
5.	SMALL SIGNAL STABILITY ANALYSIS OF SHIPBOARD POWER SYSTEMS	51
5.1	Introduction	51
5.2	Methodology for Small Signal Stability.....	55
5.3	Power System Component Models	59
5.3.1	Synchronous Generator.....	59
5.3.2	Exciter.....	60
5.3.2.1	IEEE Type-0.....	60
5.3.3	Propulsion motor load.....	61
5.3.4	VSC Models.....	62
5.4	Results	62
5.5	Summary.....	65

6.	SMALL SIGNAL STABILITY ANALYSIS ENHANCEMENT	66
6.1	Introduction	66
6.2	Participation Analysis.....	66
6.3	Static VAR Compensator (SVC).....	67
6.4	IEEE Type-1 Exciter	70
6.5	Power System Stabilizer.....	72
6.6	Summary.....	75
7.	CONCLUSIONS AND FUTURE WORK.....	76
7.1	Conclusions	76
7.2	Future Work.....	79
	REFERENCES	80

LIST OF TABLES

Table		Page
5.1	Critical eigenvalues related to MVAC and MVDC systems with Type-0 exciters	65
6.1	State participation factor to critical mode for the MVAC system with Type-0 exciter	67
6.2	Few critical Eigenvalues	75

LIST OF FIGURES

Figure	Page
2.1 NGIPS Technology development Roadmap [1].	6
2.2 MVAC architecture for shipboard power system [1, 5].	8
2.3 Proposed Notional MVDC architecture for shipboard power system [5].	9
2.4 HVDC Transmission with Line commutated CSCs [9].	12
2.5 HVDC Transmission with Forced commutated VSCs [9].	12
2.6 A Typical Voltage Source Converter [12].	13
2.7 Switching signal produced using PWM technique [19].	14
2.8 Top: Two level VSC[20] Bottom: Representation of two level voltage of a VSC [21].	16
2.9 Top: Three level VSC[20] Bottom: Representation of three level voltage of a VSC [21].	17
2.10 A Typical VSC-HVDC system [23].	20
2.11 Equivalent circuit of a Voltage Source Converter [12].	21
2.12 An example MTDC system [28].	22
3.1 Classification of Power System Stability [2].	27
4.1 A Typical two-terminal VSC-HVDC system.	35
4.2 DC Voltage control diagram of VSC [10, 35].	38
4.3 Top: Active Power Control for VSC [36]. Bottom: Reactive Power Control for VSC [36].	39
4.4 A Two-terminal VSC-MVDC system.	43

4.5	Top: Voltage across the DC link (rectifier end). Bottom: Voltage across the DC link (inverter end).....	44
4.6	Load voltage for two-terminal VSC-MVDC.....	45
4.7	A Multi-Terminal Ring Structure of MVDC system.....	46
4.8	VSC1 Subsystem MATLAB Simulink diagram.....	47
4.9	Top: Voltage across the DC link (rectifier end) for the MTDC system. Bottom: Voltage across the DC link (inverter end) for the MTDC system.....	48
4.10	Load voltage for the MTDC System.....	48
4.11	Rotor angle deviation of Synchronous machine 2.....	49
4.12	Rotor angle deviation of Synchronous machine 2 (fault applied).....	50
5.1	Power transfer in a two machine system [33].....	52
5.2	Idealized model for a two machine system [33].....	52
5.3	Eigenvalues for MVAC architecture with Type-0 exciter.....	63
5.4	Eigenvalues for MVDC architecture with Type-0 exciter.....	64
6.1	Block diagram of a SVC [45].....	68
6.2	Eigenvalues for MVAC architecture with Type-0 exciter and SVC [20]MVAR] at load bus.....	69
6.3	IEEE Type-1 exciter [42].....	70
6.4	Eigenvalues for MVAC architecture with Type-1 exciter.....	71
6.5	Eigenvalues for MVDC architecture with Type-1 exciter.....	72
6.6	Block diagram of Power System Stabilizer [38].....	73
6.7	Eigenvalues for MVAC architecture with PSS.....	74

LIST OF ACRONYMS

AC	Alternating Current
DC	Direct Current
IPS	Integrated Power System
MVAC	Medium Voltage Alternating Current
HFAC	High Frequency Alternating Current
MVDC	Medium Voltage Direct Current
VSC	Voltage Source Converter
CSC	Current Source Converter
HVDC	High Voltage Direct Current
MTDC	Multi Terminal Direct Current
NGIPS	New Generation Integrated Power System
PCM	Power Conversion Module
PDM	Power Distribution Module
PWM	Pulse Width Modulation
SPWM	Sinusoidal Pulse Width Modulation
GTO	Gate Turn- OFF Thyristor
IGBT	Integrated Gate Bipolar Transistor
IGCT	Integrated Gate Commutated Thyristor
MOS	Turn-Off Thyristor
PST	Power System Toolbox
PI	Proportional Integral
LEV	Left Eigenvector
REV	Right Eigenvector
SVC	Static VAR Compensator
PSS	Power System Stabilizer

CHAPTER 1

INTRODUCTION

1.1 Introduction

Proper design and implementation of electrical power system for the shipboard is of utmost importance because of the requirement of its compact structure. The major difference with a terrestrial power system is that all the generators, transformers, power conversion modules, loads, transmission cables and circuit breakers, on the shipboard system have to be accommodated within a small area. Power system architecture for an electric ship, should also consider several key issues regarding its stability, survivability, reliability and protection. The load variations, generation changes and effects of faults should be studied to understand the stability of the shipboard power system. The shipboard power system can be divided into several zones for load placement, and the use of circuit breakers to isolate the faulted sections will be helpful in identifying protection issues. In order to enhance the survivability of the ship, high power demanding loads like rail guns and other pulsed load may be used and the power distribution can be either AC or DC to efficiently meet the load demands.

1.2 Shipboard Power System Architectures

The most important aspect in the design of a shipboard electric power system is the survivability and continuity of electrical power supply. Survivability refers to the ability of the shipboard power system to provide support to a predetermined level, even

under attack. Continuity of electrical supply refers to the ability of the distributed systems to supply the loads during normal conditions. To meet the increasing load demands, the US Navy has been investing on ship designs with Integrated Power Systems (IPS) architecture [1] that can provide electric power to the loads from a common source.

The New Generation Technology Development Roadmap [1] presents the following architectures as possibilities to meet the power requirements of the ships for the United States Navy.

- i) Medium Voltage AC (MVAC) System
- ii) High Frequency AC (HFAC) System
- iii) Medium Voltage DC(MVDC) System

Each of these architectures has a particular significance. For example, MVAC architecture is preferred in ships where the power density is not so high. HFAC provides the advantage of decreased cross sectional area due to the increased frequency of operation. MVDC architecture is preferred for power dense loads. The operating voltages and power levels may be different for these architectures. A detailed introduction for these architectures is given in chapter II.

1.3 Stability Studies

Stability is an important consideration for the safe and secure operation of any power system. The study of stability requires the knowledge of the factors causing instability. In a power system, whether terrestrial or shipboard, instability can be caused due to a number of factors, like loss of generation, component failure or system faults. In some cases, a prolonged fault condition may lead to a severe problem. For example,

voltage collapse, which is a local phenomenon, may lead to voltage instability after a series of events. The classification of stability problem [2] is helpful in determining the reason for instability and formulate a method to mitigate its effects. When formulating a control measure, the overall stability of the system should be ensured.

1.4 Objective of Thesis

As described earlier, stability studies are necessary before the implementation of any architecture proposed in [1]. The MVDC architecture, which has the capability of supplying power dense loads, employs power electronic devices for power conversion. This will add further to the complexity of the shipboard power system stability study.

In general, based on the factors causing instability, the stability problem can be classified as

- i) Rotor Angle Stability
- ii) Frequency Stability
- iii) Voltage Stability

These are clearly explained in chapter III. These three classifications are concerned with different aspects of the stability problem but they are closely related to one another. This thesis work concentrates specifically on the rotor angle stability of the MVDC shipboard power system. Rotor angle stability can be further classified into small signal and transient stability based on the amount of disturbance. The objective of this thesis is to look at the small signal as well as transient stability of the simplified MVDC shipboard power system. To fulfill the objective, a two-terminal VSC-MVDC system will be first implemented. This was done to gain some confidence on the working of a VSC-

MVDC system and to observe the performance of the voltage regulator and the power dispatcher. This will be extended to a VSC-MTDC system depicting the shipboard power system and the transient behavior with a three- phase fault at one of the generator terminals will be studied. Small signal stability analysis will be carried out on the MVDC as well as MVAC architectures to make a comparison in the critical damping ratios.

1.5 Thesis Outline

Chapter II gives an overview of the shipboard power system architectures. Background work on Voltage Source Converter based High Voltage Direct Current (VSC-HVDC), Multi-Terminal DC (MTDC), advantages and applications of the VSC-HVDC are also described in this chapter. Problem statement and its formulation are described in Chapter III. Chapter IV concentrates on the modeling and transient stability analysis of VSC-MVDC systems. The power system component models used and the small signal stability work on MVDC system are presented in Chapter V. Chapter VI presents the studies related to the control of small signal instability of the system. Chapter VII presents the main conclusions of the thesis and outlines few scope for future research work in this area.

CHAPTER 2

BACKGROUND AND LITERATURE REVIEW

2.1 Introduction

U. S Naval ships had conventionally employed 450V, 60 Hz AC radial distribution systems with multiple generators connected to separate switchboard panels and employed for distribution to the load centers. In order to enhance survivability of the system, zonal distribution systems, having two main buses at starboard and port levels, have been suggested [3]. The zonal Medium Voltage AC (MVAC) distribution system [1,4] will employ three-phase 60 Hz, AC system at 4.16 kV using a high- impedance ground (This operating voltage may reach 6.9kV or 13.8 kV in the near future). These voltage levels are dependent on the available ratings of switches for effective isolation during normal and fault conditions. The zonal MVAC scheme is preferred if the load power density is not very high. Next generation ships will employ advanced missiles, weapons, and rail guns to improve their survivability. All these services/components can be added to the ship keeping in mind its compact structure and weight. To support these high power demanding loads, the following two alternative distribution schemes have been recently proposed [1].

- a. High Frequency AC (HFAC) distribution
- b. Medium Voltage DC (MVDC) distribution

A technology development roadmap [1] is shown in figure 2.1. MVAC architecture is an ideal choice for ships whose load requirements are not very high.

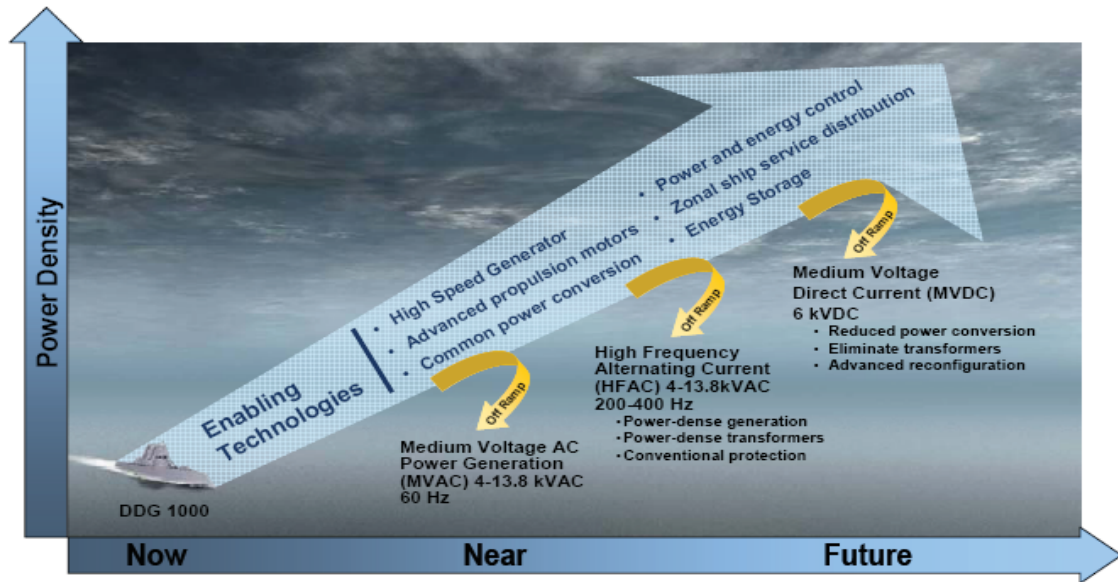


Figure 2.1 NGIPS Technology development Roadmap [1].

In the HFAC architecture, the operating frequency is in the range of 60 Hz to 400 Hz, with a supply voltage of 4.16 kV using a high-impedance ground. The advantages [1] of high frequency operation include:

- i) Great reduction in the cross sectional area of the transformer core.
- ii) Reduction in harmonic filters.

The major difference between MVDC over MVAC or HFAC distribution is that the power distribution takes place at medium level voltages of ± 3000 VDC to ± 10000 VDC using a high- impedance ground. Some of the advantages [1] include:

- i) Fault current levels are low as compared to the AC systems.

- ii) No skin effect which leads to reduction in the weight of cables.

Moreover, MVDC is a compact and power dense architecture for high power demanding electric loads.

All of the above three architecture have their own advantages and disadvantages. Load requirements, ease of implementation, cost of the equipments used in a particular architecture (For example, converters used in MVDC architectures are costly), design of components (For example, DC circuit breakers for high power ratings are not available) and many others issues should be effectively addressed before the implementation of any architecture. The New Generation Integrated Power System (NGIPS) roadmap tries to address some of these issues based on time span.

2.2 Zonal Shipboard Power System Architectures

For improved survivability of shipboard power systems, there has been a move from radial distribution systems to zonal distribution systems. As the name indicates, the loads are distributed in several zones. These zonal distribution systems for MVAC and MVDC architectures are described below.

2.2.1 MVAC architecture:

A shipboard power system with MVAC architecture [1, 5] is shown in Figure 2.2. It has two main generators of 36 MW each and two auxiliary generators, each of 4 MW rating connected through a 4.16 kV AC bus. The entire architecture is divided into five zones for load distribution, placement of Power Conversion Modules (PCMs), converters, and Power Distribution Modules (PDMs).

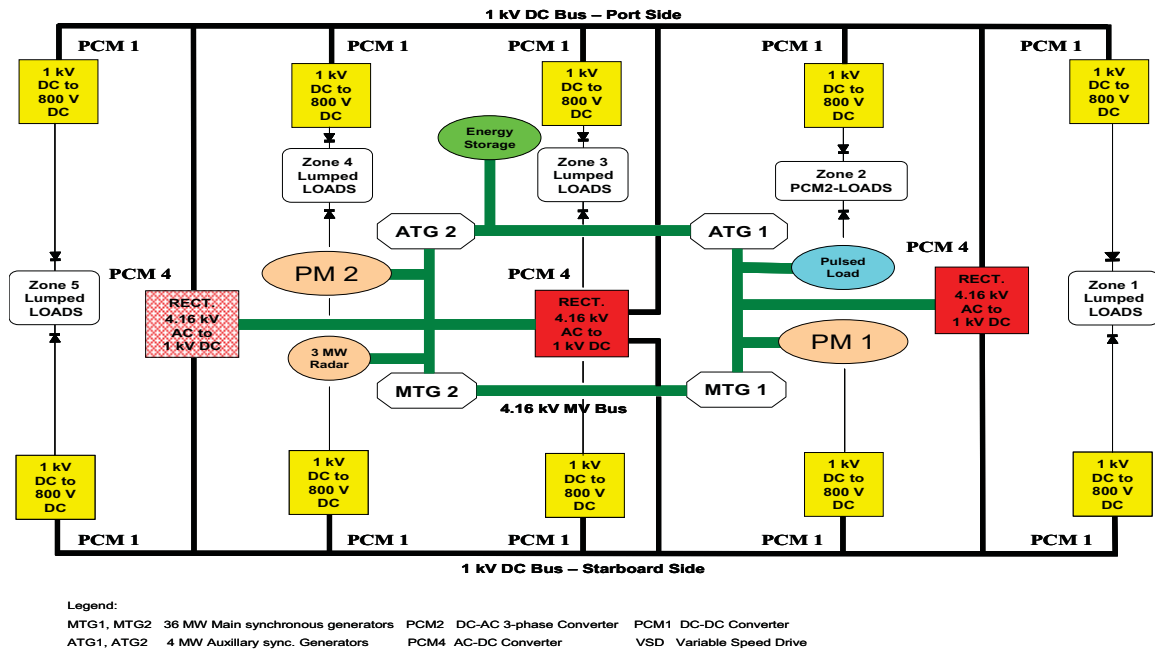


Figure 2.2 MVAC architecture for shipboard power system [1, 5].

The loads on the shipboard power system include two propulsion motors of 36.5 MW each, 3 MW radar load, pulsed loads and the rest represented by lumped load. The power conversion modules (PCMs) are required to supply the DC loads operating at different voltage levels. PCM-4s are used to rectify the 4.16 kV AC voltage to 1 kV DC for powering the port and starboard buses, as shown in Figure 2.2. PCM-1s are used to step down the 1 kV DC voltage to 800 V DC to supply any DC load operating at that voltage. PCM-2s are used to convert 800 V DC to 120/208 V AC to supply AC loads. This architecture also includes energy storage devices connected at the 4.16 kV AC bus.

2.2.2 MVDC Architecture

This architecture is proposed in [5]. In the MVDC architecture, the power may be distributed at voltages ranging from ± 3000 V DC to ± 10000 V DC. The notional MVDC

architecture employs a 5 kV DC ring bus, connected to four converters and supplied through four synchronous generators. Among these generators, two 36 MW generators (MTG1 and MTG2) are designated as main generators and the other two 4 MW generators act as auxiliary generators (ATG1 and ATG2). The MVDC architecture is shown in Figure 2.3. This architecture is also divided into five zones for the placement of loads, PCM's and PDMs. Power conversion modules operate at different voltage levels as compared to the MVAC architecture. PCM-4 is used to rectify the 4.16 kV AC to 5 kV DC, which feeds the DC ring bus (port and starboard side). PCM-1 is used to step down this 5 kV DC to a suitable voltage required by the loads. Loads requiring AC power at 4.16 kV are supplied with the help of PCM2. The architecture also accommodates energy storage devices like capacitors and fuel cells. It also consists of rail guns and a radar array.

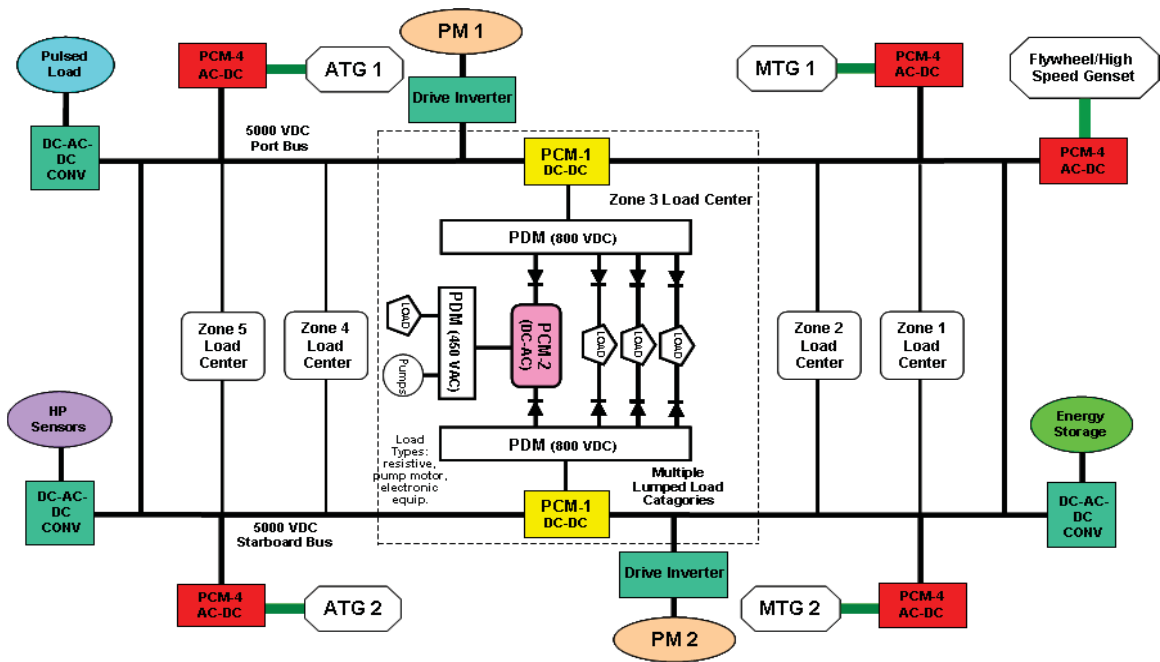


Figure 2.3 Proposed Notional MVDC architecture for shipboard power system [5].

The MVDC distribution is drawing more attention after development of Voltage Source Converters (VSC) and successful implementation of the VSC based multi-terminal HVDC systems.

2.3 Literature Review on VSC based HVDC

The concept of HVDC transmission in electric power systems offers the following advantages [6, 7].

- i) Connecting two grids operating at different frequencies.
- ii) Long distance power transmission.
- iii) Underwater cables, where AC transmission is impractical because of high capacitance of cables and requires immediate compensating stations.

HVDC, based on thyristor commutated converters, has been used for many years [6]. With the developments in semiconductor technology and their increased power rating, VSC-HVDC based on Insulated Gate Bipolar Transistors (IGBTs) serves as a potential technology for DC power transmission, specifically in multi terminal configurations. Proper control algorithms are implemented to fully exploit the capabilities of VSC-HVDC. Different control algorithms for VSC-HVDC have been analyzed in [8]. In [9], PWM based control of three level VSC has been utilized. Optimization of the controller parameters and control scheme using Sinusoidal Pulse Width Modulation (SPWM) is explained in [10]. Inter-area decoupling and local area damping by VSC-HVDC are studied in [11].

In a two-terminal VSC-HVDC transmission, one converter acts as a voltage regulator and the other acts as power dispatchers [12]. The voltage regulator maintains

the voltage across the DC bus to a reference value and the power dispatcher regulates the real power through the bus.

Commercial applications of VSC-HVDC include HVDC Light by ABB group [13] and HVDC plus by Siemens [14]. HVDC Light was introduced in 1997 with underground transmissions up to 350 MW in operation. In the upper range, HVDC Light is implemented for 1200 MW and ± 320 kV [13]. One of the planned commercial applications of HVDC plus is the Trans Bay Cable Project [15], which has a power rating of 400 MW with DC voltages at ± 200 kV and a DC current of 1000 Amps. The transmission system consists of two converter stations, the San Francisco Converter Station and the Pittsburg Converter Station, connected by a submarine/onshore HVDC cable system . Some more commercial applications include Gotland HVDC for small scale DC transmission [16] and Tjaerobore project for connection to a wind farm [17].

2.4 Voltage Source Converter

Earlier High Voltage Direct Current (HVDC) transmission used line commutated Current Source Converters (CSCs). In CSCs, the DC current always has one polarity and the power reversal is achieved through the reversal of DC voltage polarity [18]. These devices can be turned-on with the help of a gate signal and the turn-off cannot be controlled. This happens only when the current crosses zero. Hence, the conventional thyristor-based converters can only be CSCs because of lack of turn-off capability. CSC based HVDC transmission is shown in figure 2.4.

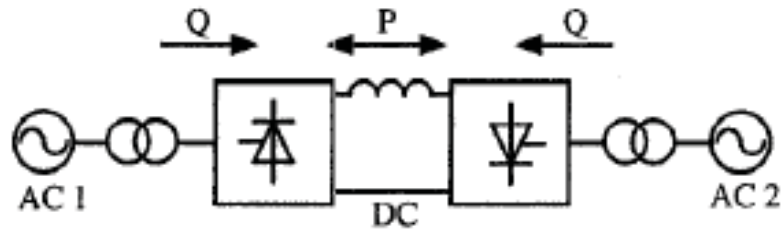


Figure 2.4 HVDC Transmission with Line commutated CSCs [9].

The turn-off capability is achieved with the help of devices like Gate Turn- Off Thyristor (GTO), Integrated Gate Bipolar Transistor (IGBT), Integrated Gate Commutated Thyristors (IGCT) and MOS Turn- off Thyristor (MTO). These devices are force commutated. In VSCs, the DC voltage always has one polarity, and the power reversal is achieved through the reversal of DC current polarity [18]. IGBT based devices can be either used for CSC or VSC. VSC based HVDC transmission is shown in figure 2.5.

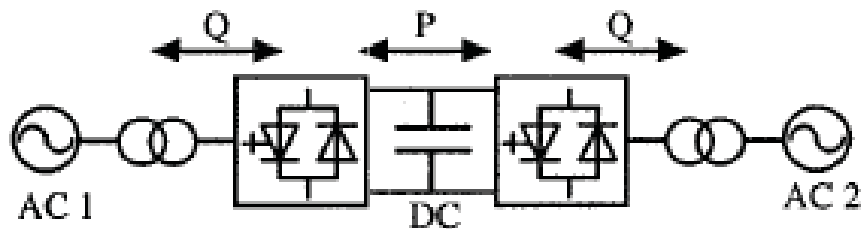


Figure 2.5 HVDC Transmission with Forced commutated VSCs [9].

Forced commutated VSCs also have the following advantages over line commutated CSCs [9]

- i) Independent control of active and reactive power.
- ii) Faster response due to high switching frequency.
- iii) No commutation failure problem.

Voltage source converter, the important component of VSC-HVDC, is briefly explained and is shown in figure 2.6. The DC voltage across the capacitor ends and the switching action of the converter switches produces the three-phase AC voltages $v_a(t)$, $v_b(t)$, and $v_c(t)$. The DC voltages and the AC voltages are related through a switching function. This switching function depends on the modulation technique used to turn ON-OFF the switching devices.

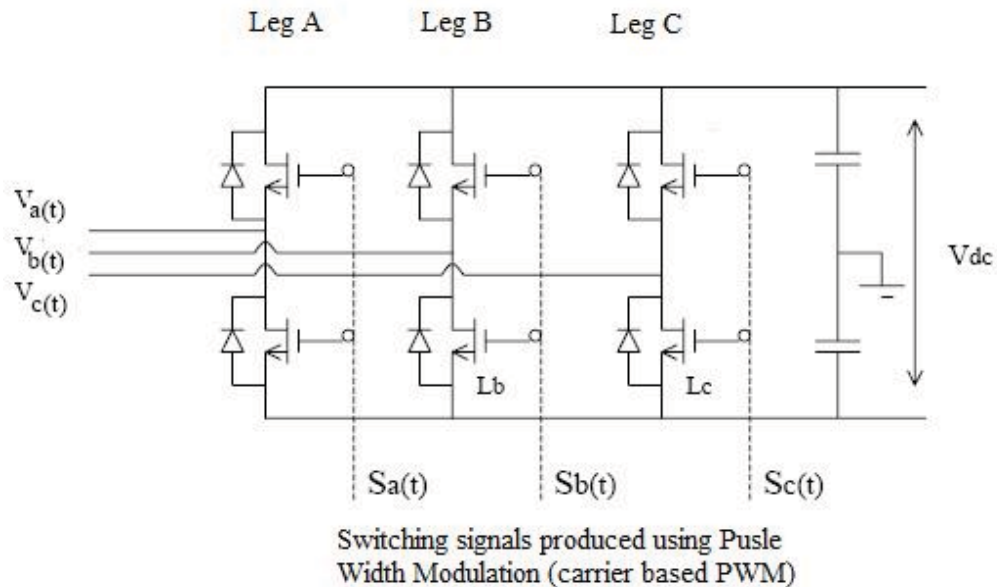


Figure 2.6 A Typical Voltage Source Converter [12].

The grounded DC voltage with respect to midpoint and the three-phase AC voltages [19] can be written as:

$$v_a(t) = 0.5 S_a(t) V \quad (2.1)$$

$$v_b(t) = 0.5 S_b(t) V \quad (2.2)$$

$$v_c(t) = 0.5 S_c(t) V \quad (2.3)$$

The switching signal for the VSC can be generated using any one of the pulse width modulation techniques (carrier based PWM, Space vector etc). The modulating signal, corresponding to each phase, is generated using the switch function signal S_a . These switching signals are used to trigger the switching devices in each phase to produce the three phase voltages. The switching signal and modulating signals are shown in figure 2.7.

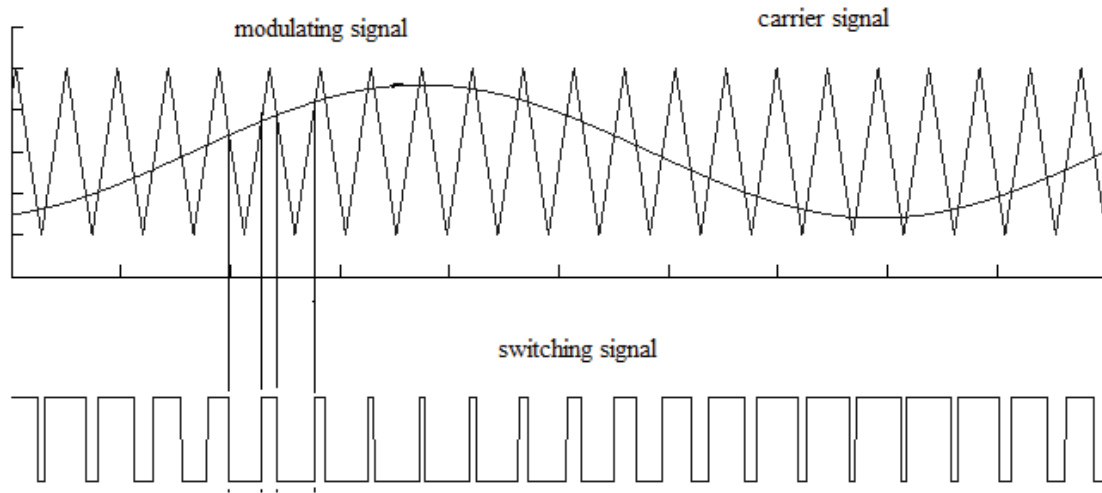


Figure 2.7 Switching signal produced using PWM technique [19].

The relation between the switching signal and the modulating signal when the high frequency harmonics are filtered, is given as

$$S_a(t) = m_a(t) \quad (2.4)$$

where K is a constant

Hence, the a- phase filtered voltage can be written as

$$v_a(t) = 0.5 K m_a(t) V \quad (2.5)$$

The modulating signal can be modified further to have the form

$$m_a(t) = M \sin(\omega t - \alpha) \quad (2.6)$$

The three- phase voltages on the AC side can be finally written as

$$v_a(t) = 0.5 K M \sin(\omega t - \alpha) V \quad (2.7)$$

$$v_b(t) = 0.5 K M \sin(\omega t - \alpha - 120^\circ) V \quad (2.8)$$

$$v_c(t) = 0.5 K M \sin(\omega t - \alpha + 120^\circ) V \quad (2.9)$$

For high power applications, VSC has two configurations, as explained below.

2.4.1 Two level VSC

A three phase forced commutated VSC can be easily built using a two level bridge (requires minimum number of components). As the name suggests, the output voltage on the ac side has two levels +V_{dc} and -V_{dc}. It is composed of valves, which is a combination of a number of series connected turn-off devices and anti parallel diodes. The two level VSC and its output were shown in figure 2.8.

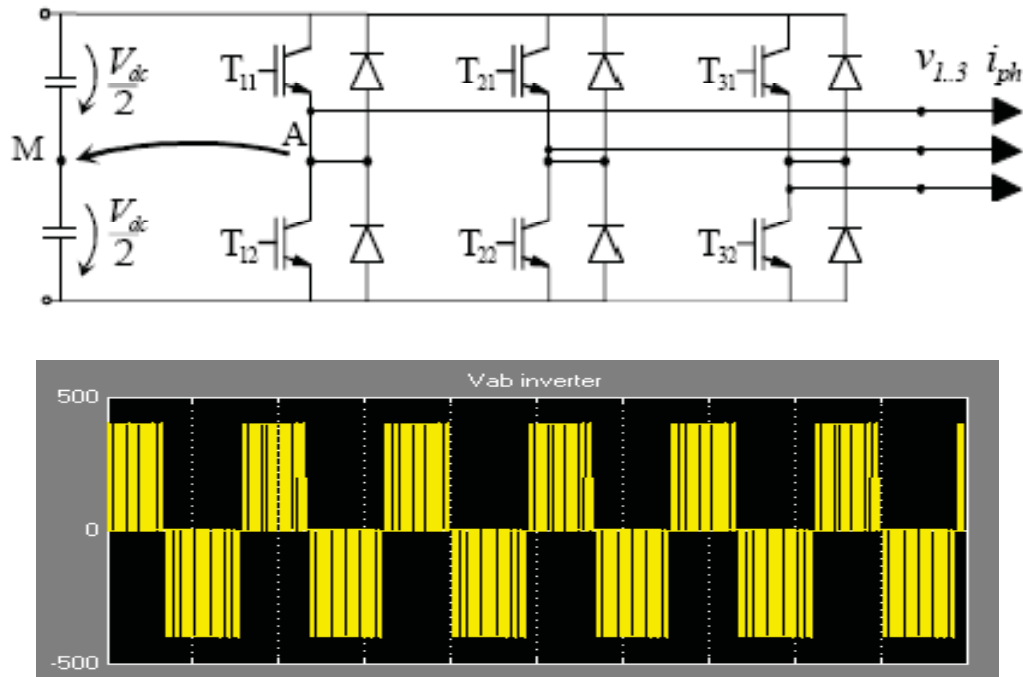


Figure 2.8 Top: Two level VSC[20] Bottom: Representation of two level voltage of a VSC [21].

2.4.2 Three level VSC

Three level VSC, also called NPC (Neutral Point Converter), is preferred for high power applications. Its output is modulated in three levels - $V_{dc}/2$, 0, $+V_{dc}/2$ instead of two. The three level bridge and its output voltage are shown in figures 2.9 (a) and (b), respectively. The three level bridge is different from the two level bridge with respect to the additional diodes on the DC side. There are also six extra valves, as shown in the figure 2.9. The three level VSC and its output were shown in figure 2.9. Even for high power applications, the three level bridge configuration will remain the same.

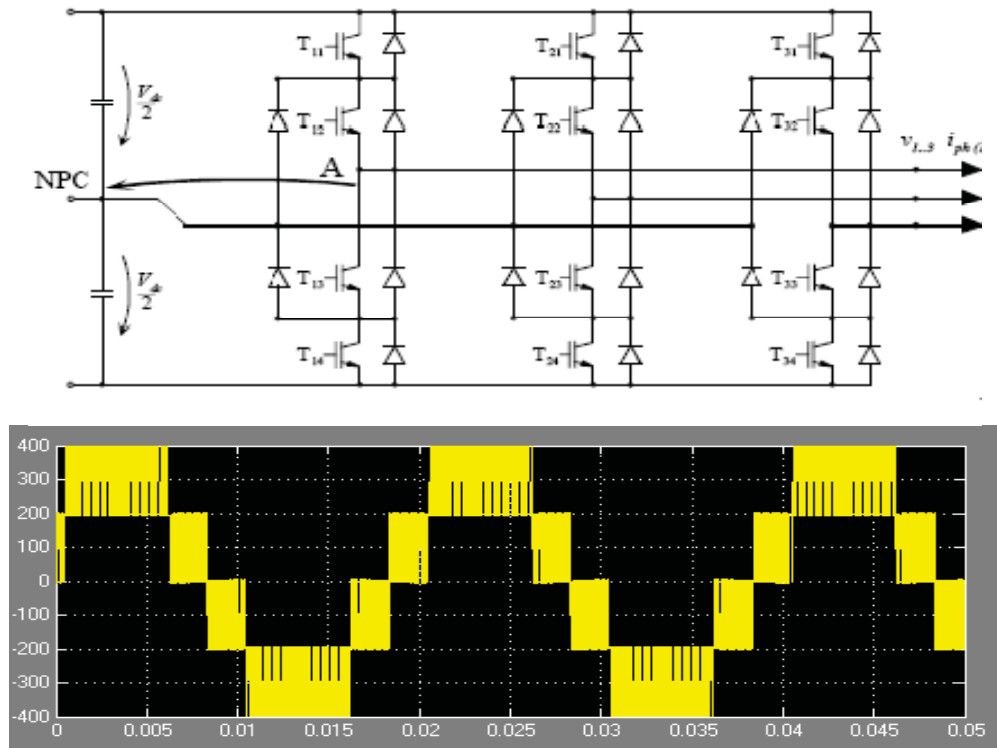


Figure 2.9 Top: Three level VSC[20] Bottom: Representation of three level voltage of a VSC [21].

The three level bridge has the following advantages [20, 22]:

- i) Lower insulation stress in cables because of three level voltages.
- ii) Higher DC bus voltage.
- iii) Lower switching losses for the same output waveform quality.

Some disadvantages include unequal DC voltages across capacitors and a larger number of components.

2.5 VSC-HVDC System

A typical VSC-HVDC system consists of the following components [12].

2.5.1 Converters

The IGBT based converter, in a VSC-HVDC system, acts as a rectifier or inverter based on the power flow. The converter can be either two level or three level, based on the rated power to be handled by the system.

2.5.2 Converter Transformers

The purpose of the converter transformer is to maintain equal voltage on the AC system side and the converter AC side. The reactance of the transformer also contributes to the phase shift between these two AC voltages. The winding configuration is selected based on the predominant harmonics that may be produced by the power electronic devices in the system. Generally, with VSC converters, the wye grounded/ delta configuration is preferred. The wye ground connection on the primary side provides a path for the zero sequence currents to flow through ground whenever there is an AC side fault. The delta connection on the secondary side of the converter transformer is grounded at the DC capacitor midpoint. The zero-sequence currents on the VSC side are localized within the winding and do not propagate to the connected system.

2.5.3 AC Filters

The converter currents and voltages are not sinusoidal due to the valve switching process occurring in IGBTs. Along with the fundamental frequency AC component, these non-sinusoidal currents and voltages contain higher-order harmonics. Therefore, AC filters are needed in the VSC-HVDC scheme to filter out these harmonics. The generation of AC harmonics depends on the following factors.

- i) Type of modulation (sinusoidal PWM, space vector etc.)

- ii) Modulation index (m) (Converter output voltage/ DC voltage)
- iii) Frequency index(p) (Carrier frequency/ modulator frequency)

These filters are, generally, connected as shunt elements on the converter AC side. High pass filters or tuned filters can be used to filter these high frequency harmonics. With carrier frequency of 2250 and modulator frequency of 50 Hz, the frequency index (p) = 45, shunt AC filters are required to filter out 45th and 90th harmonics. AC filters also supply a certain amount of reactive power based on the converter rating.

2.5.4 Phase Reactors

The phase reactor helps in providing the necessary phase angle between the system AC voltage and the converter AC voltage. It is also essential to control the flow of active and reactive power between the AC system and DC link. The value of the phase reactor has a significant impact on the power flow, because it produces the desired shift between the two AC voltages.

2.5.5 DC Capacitors

A DC capacitor acts as an energy buffer to control the power flow and DC voltage ripple. PWM switching of converters results in harmonics with the current flowing on the DC side. To prevent the ripple in the DC voltage, a capacitor of suitable rating is desired. The capacitor rating should be small to achieve fast converter response. Generally the capacitor size is defined [23] as τ ,

$$= \sqrt{\frac{1}{2} \frac{CV_{dc}^2}{VS_{nomV}}} \quad (2.10)$$

where,

C is the DC capacitance.

V_{dc} is the DC side voltage.

S_{nom} is the nominal apparent power of the converter.

The time constant is defined as the time taken to charge the capacitor to the base voltage through its base current. The smaller the time constant, the faster the control of active and reactive power flows.

2.5.6 DC Cables

Two converter stations are generally connected through DC cables. The DC cables are chosen such that the insulation material is strong enough to withstand the DC voltages. Extruded DC cable technology [24] may emerge as a cost effective technology compared to a mass-impregnated cable or oil-filled cable. This is not suitable to thyristor based HVDC because of its sensitivity to voltage reversal. In VSC-HVDC, the voltage polarity remains unchanged and the power reversal is achieved through the reversal of the current polarity. Hence, an extruded DC cable technology can be recommended for the VSC-HVDC. A typical VSC-HVDC system is shown in figure 2.10.

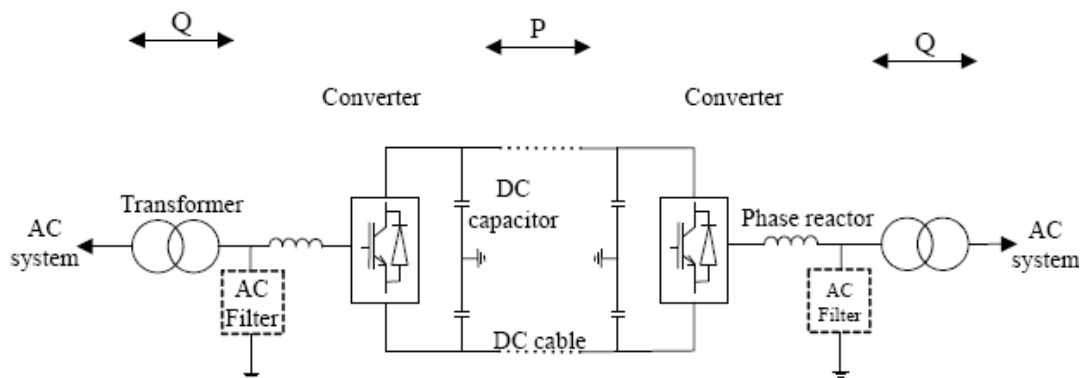


Figure 2.10 A Typical VSC-HVDC system [23].

2.6 Concept of Multi-Terminal DC

The equivalent circuit of a VSC [12] consists of i) an ideal voltage source in series with each of the three phases ii) an ideal current source on the DC side and iii) instantaneous real power balance of all the ideal current sources and ideal voltage sources. It is shown in figure 2.11.

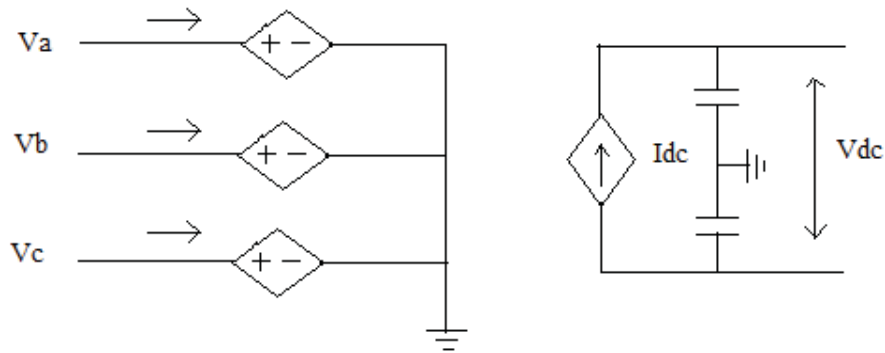


Figure 2.11 Equivalent circuit of a Voltage Source Converter [12].

Voltage source converters are modeled as ideal current sources on their DC sides and can be connected in parallel across a pair of DC buses. This characteristic of the VSC brings the concept of Multi Terminal DC.

The Multi-Terminal DC (MTDC) system is an extended version of the two-terminal VSC-HVDC. This concept increases the functionality and applications of two-terminal VSC-HVDC system. A typical example of MTDC system is shown in Figure 2.12.

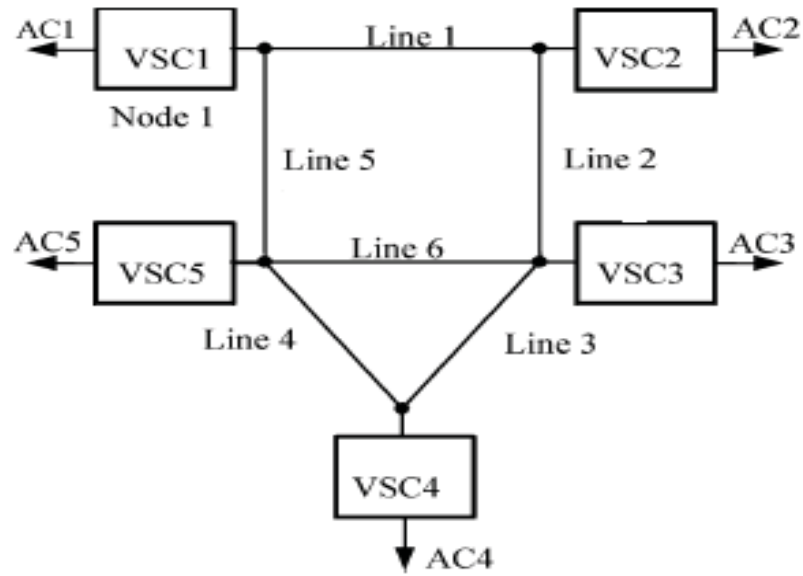


Figure 2.12 An example MTDC system [28].

Several works have been done on MTDC systems. The MTDC system has N voltage- source converter stations connected to a DC bus, in which one VSC station operates as a DC voltage regulator to control the DC voltage across the bus which is set to a particular reference value. The rest of the VSC stations act as power dispatchers and the DC voltages across their terminals is equal to a value, which is obtained by subtracting the drop across the line from the reference value. Work has been done in [25] to design a control system to maintain the DC voltage within a narrow range of 5% during the event of loss of one VSC station (except the DC voltage regulator). Multi-terminal LVDC system for optimal power acquisition has been presented in [26]. Optimal acquisition and aggregation of offshore wind power by MTDC has been discussed in [27]. ABB is trying to commercialize this concept of Multi-terminal DC by the name Multi Terminal HVDC Light grid.

2.7 Advantages and Applications of VSC-HVDC

The high controllability of VSC-HVDC offers the following advantages [29]:

- i) VSC-HVDC has the ability to control the active power and reactive power independently by making use of pulse width modulation. One converter controls the dc bus voltage, whereas the other converters control the active power.
- ii) Reactive power generated and consumed by a converter can be used for voltage control/ stability improvement applications to meet the needs of the connected network.
- iii) Each VSC has four control modes, viz active power control, reactive power control, DC voltage control and AC voltage control. The use of any particular control depends on the specific application.
- iv) Enhanced power quality is achieved through reactive power supply capability of VSC-HVDC, which helps in maintaining the AC voltage in the system. Reactive power support from the VSCs also helps in minimizing the harmonics.
- v) Thyristor based HVDC suffers from commutation failure due to disturbances in the AC system. This problem no longer exists in VSC-HVDC due to self commutated devices used in the VSC.
- vi) Communication between converter stations is not needed as they operate independently and, hence, the speed and reliability of the controller are improved.
- vii) It has ability to add links to expand operation. i.e. the concept of Multi-terminal DC.
- viii) It has ability to add energy storage devices, like a bank of capacitors and batteries.

- ix) Construction and installation costs are less due to its compact size and volume.
- x) It has low maintenance and service costs.

Some of the applications of the VSC-HVDC are as following

- i) Power quality can be improved in industrial plants with and without on-site generation supplied through VSC-HVDC [30].
- ii) Optimal acquisition of wind power in distant offshore wind farms where submarine transmission of electric power is preferably DC [27].
- iii) In large cities where the distribution systems are often served by underground cable systems, VSC MTDC proves to be a good alternative to supply premium quality power in view of safety and environmental reasons [31].
- iv) It can be used to enhance the power system stability [32].

2.8 Summary

This chapter has given an overview of the zonal shipboard power system architectures as MVAC and MVDC architectures are explained in detail. Some background work on VSC-HVDC, along with overview of VSC and its configurations are provided. Components of VSC-HVDC system are discussed. The equivalent circuit of the VSC, the concept and characteristics of Multi-Terminal DC, background work on VSC-MTDC, and its commercial applications are briefly explained. Advantages and applications of VSC-HVDC are also briefly described.

CHAPTER 3

PROBLEM STATEMENT AND DESCRIPTION

3.1 Introduction

The advantages of MVDC architecture over the MVAC architecture for the shipboard power system have already been discussed in chapter II. The high power ratings of IGBT based VSCs and their successful implementation in many applications prove that the VSCs are a good choice to achieve the required DC voltages for the proposed MVDC ring architecture. From the equivalent circuit of VSC, shown in chapter II, it can be understood that a VSC can be represented as an ideal current source which allows the parallel connection of VSCs. The DC ring structure, proposed in [5] is fed by four generators, is connected through VSC converters forming a ring bus and has been implemented with this feature of the VSCs.

3.2 Problem Statement

Design of a shipboard power system becomes complex because of small size and reduced weight requirements of its various components. All the components on the shipboard power system, like synchronous generators, propulsion motors, power conversion modules, power distribution modules and circuit breakers should be carefully designed to accommodate all these within a small area. The adoption of a new architecture for the shipboard power system requires investigation of several key issues related to stability, reliability, protection and cost of implementation. The proposed

MVDC architecture [5] implements DC power distribution at voltages ranging from ± 3000 VDC to ± 10000 VDC. This DC power conversion is achieved with the help of power electronic devices like IGBTs operating as VSCs. The assessment of stability of a MVDC architecture, with power electronic devices, is of great importance and has been conducted in this work.

3.3 Classification of Stability Problem

Power system stability as a whole is a single problem but it takes different forms based on the factor responsible for instability (rotor angle, frequency or voltage). The classification of the stability problem [2] is important in determining the factor/parameter causing instability. This classification also helps in devising a method to maintain the stability of the power system. The following criteria are generally considered for its classification [33]:

- i) Physical nature or main parameters responsible for causing instability.
- ii) Size of disturbance.
- iii) Time span to assess the stability of the system.
- iv) Method followed to predict stability.

Based on the above factors, the stability problem can be classified as shown in figure 3.1.

The above classification is briefly explained as following.

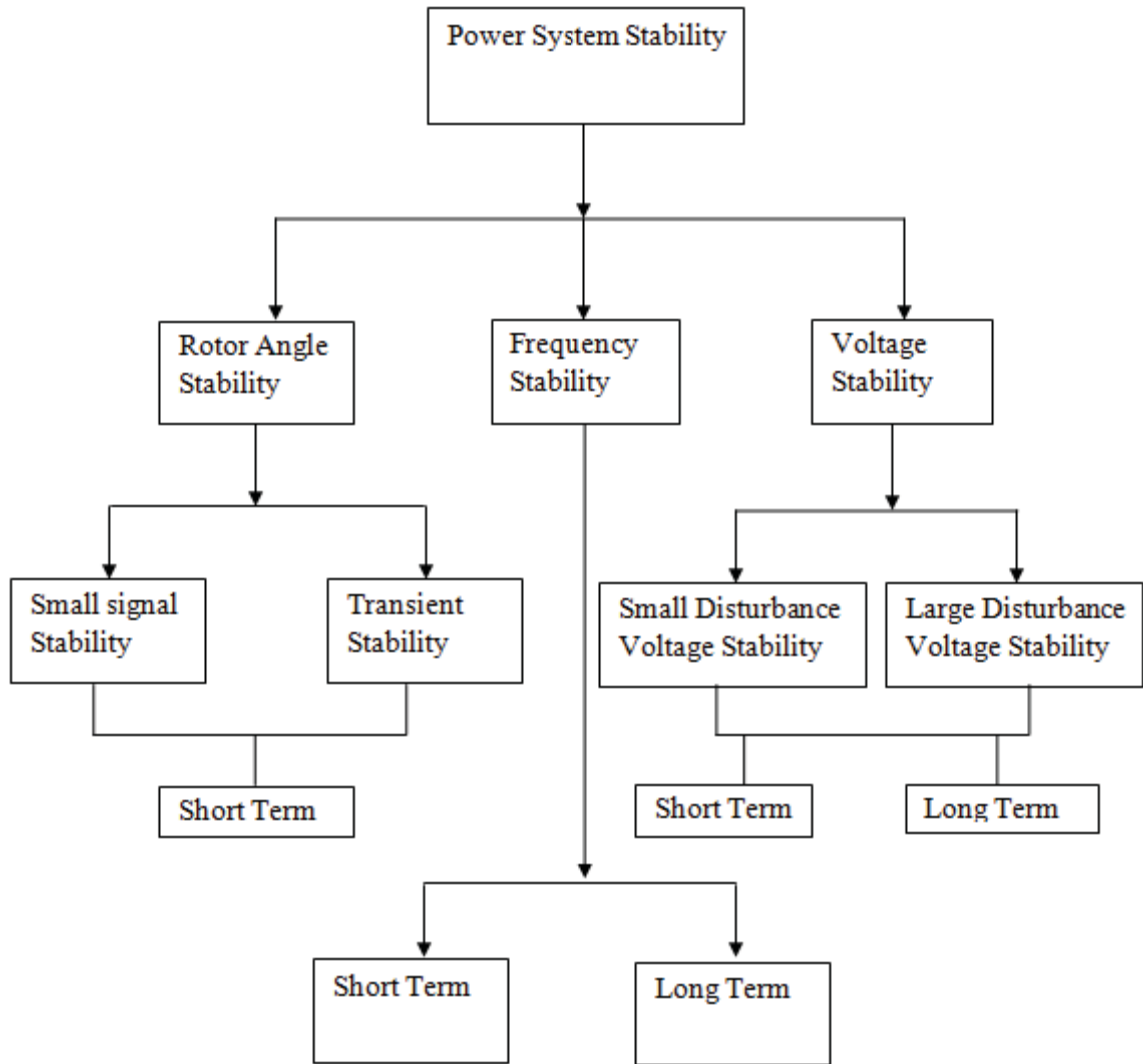


Figure 3.1 Classification of Power System Stability [2].

3.3.1 Rotor Angle Stability

Rotor angle stability refers to the ability of interconnected synchronous machines to maintain synchronism following a disturbance. This deals with the electromechanical oscillations which are always present in the power system. Rotor angle variations lead to variations in power output of synchronous machines.

The rotor angle stability can be further classified as

- i) Small signal stability

ii) Transient stability

Small signal stability is defined [2] as the ability of the power system to maintain synchronism under small disturbances which are always present in the system. These disturbances are small (For example: load and generation changes) and, hence, the system dynamical equations can be linearized for the stability analysis. Small signal instability can take the following forms: insufficient synchronizing torque leading to a steady increase in rotor angle or increasing amplitude of rotor oscillations due to insufficient damping torque. The behavior of the system to these disturbances is greatly influenced by the excitation control used. For example, the lack of an automatic voltage regulation may lead to insufficient synchronizing torque. This is further classified as Local mode, Inter-area mode, Control mode and Torsional modes which will be explained in chapter V. All these modes of oscillations arise due to a specific condition like weak tie-lines, poorly tuned exciters, poor response of speed governors, HVDC converters and their controls.

Transient stability is defined [2] as the ability of the power system to maintain synchronism when subjected to a severe or large disturbance. It involves the study of torque balance of synchronous machines following a large disturbance like three-phase faults, sudden loss of generation, or sudden damage to equipment. Under these disturbances, large variations in generator rotor angle were observed and there may also be a shift in the steady-state operating point (different from the initial operating point) following a disturbance.

Both the small signal and transient stability can be further classified as a short term stability problem based on the time frame taken for the study.

3.3.2 Frequency Stability

This corresponds to the dynamic response of the system to severe swings in frequency. This has to be carefully addressed because such huge swings in frequency is not desirable for the safe operation of the power system. This has been further classified into short term and long term, based on the time span of the phenomenon and the time considered to assess the stability.

3.3.3 Voltage Stability

Voltage stability is defined [2] as the ability of a power system to maintain steady state voltages at all the buses during normal conditions and also after being subjected to a disturbance. The root cause of voltage instability can be attributed to reactive power imbalance in the system. Although voltage instability is a local phenomenon, it causes a series of events to occur in the system and eventually leads to voltage collapse, which is not desired for the safe operation of power system. Voltage instability and rotor angle instability are inter-related. For example, rotor angle variations may lead to voltage instability. This is further classified as.

- i) Small disturbance voltage stability
- ii) Large disturbance voltage stability.

Small disturbance voltage stability deals with maintaining voltages following a small disturbance, such as small and gradual variations in system loads. This is dependent on the characteristics of the load and, in general, can be viewed as the system voltage response to small changes.

Large disturbance voltage stability deals with maintaining voltages following large disturbances, like line to ground faults, critical damage to equipment or other system contingencies arising suddenly. This requires looking at the dynamic response of a system over a satisfactory time interval (few seconds to tens of minutes). In short it can be explained as the ability to maintain voltages at all the buses following a disturbance and following system- control actions.

The time span in the above classification [33] is given below:

- i) Short- term/ Transient- 0 to 10 seconds
- ii) Mid- term-10 seconds to a few minutes
- iii) Long-term- a few minutes to 10s of minutes

The above classification of power system stability provides a chance to look at the parameter causing instability and take necessary action to improve the overall system stability.

3.4 Problem Description

The stability studies of MVDC architecture are helpful in gaining a thorough understanding of the behavior of the system to variations in loads, generation and system faults, in the presence of power electronic devices. The work presented in this thesis is concerned particularly with the rotor angle stability of the shipboard power system, i.e. small signal stability and transient stability for the proposed MVDC architecture.

3.4.1 Transient Stability

To carry out the transient stability analysis on MVDC architecture, a two-terminal VSC-MVDC was first implemented. The two-terminal VSC-MVDC system has one of

the converters controlling the voltage across the DC bus and the second converter taking care of active and reactive power control. This concept has been extended to a Multi-terminal DC ring structure. The MTDC structure considered is similar to the MVDC architecture for the shipboard power system, which has been simulated in MATLAB Simulink as explained in chapter IV. Among the three converters, in the MTDC ring structure, one converter acts as DC voltage controller and the other two act as Power dispatchers. The ratings of the converter transformers and phase reactors have been selected such that the DC voltage across the bus is maintained at 5000 kV. A three-phase fault is applied across the terminals of one of the synchronous machines to look at the transient behavior of the MTDC system. The variation in the rotor angle of synchronous machines is presented in chapter IV. The variation of voltages across the DC bus and the load voltage are also studied in this chapter.

3.4.2 Small signal stability

The small signal stability study, presented in this thesis, has considered a linearized dynamical model of the power system around an initial operating point to analyze the stability of the MVAC as well as the MVDC architectures of the zonal shipboard power system. The models of the power system components used in this work, include a two- axis sub transient model of synchronous generator, IEEE Type-0 as well as Type-1 exciters, dynamic model of the propulsion motor load and dynamic model of steady state model of VSC, whose AC side is represented as a constant voltage source connected to the AC bus through a transformer, and the DC side as an ideal current source and dynamic model of Static VAR Compensator. All the power system component models are clearly explained in chapters V and VI. The DC side of the VSC,

being an ideal current source, allows parallel connection of VSCs across a DC bus to form the DC ring and achieving the MTDC configuration. Results obtained at a base operating condition, through AC-DC load flow, have been used as the initial operating point for linearizing the system equations. Eigenvalue analysis of the system state matrix has been carried out to assess the small signal stability of the system. Eigenvalues and the damping ratios for MVAC and MVDC architectures with Type-0 exciter are presented in chapter V.

Looking at the eigenvalues and the damping ratios corresponding to few critical eigenvalues for both the architectures, it can be understood that significant improvement can be achieved by compensating the unstable modes. The modes participating maximum to the unstable mode in the MVAC architecture can be determined using Participation analysis. From these unstable modes, corrective action can be taken. The improvement in damping ratio with a higher order excitation control, i.e. use of IEEE Type-1 exciter in place of Type-0 exciter for the MVAC and the MVDC architectures, is presented in chapter VI. The impact of placing an SVC at the load bus is also studied. A Power System Stabilizer (PSS) is also added to the system to look its impact on the damping ratio of the mode. The eigenvalues corresponding to the MVAC and the MVDC architectures with Type-1 exciter, SVC and PSS are presented in chapter VI.

Small signal stability work has been performed using Power System Toolbox (PST) developed [34] by Cherry Tree Scientific Company, Canada [34]. It builds the state matrix using a perturbation model.

3.5 Summary

This chapter discussed the problem statement focused on the assessment of the stability of the MVDC architecture of the shipboard power system. It provides an overview of the classification of the power system stability problem. All the factors/parameters affecting the stability classification are briefly explained. The implementation and the method adopted to look at the transient behavior of MTDC systems were discussed. It also discusses the approach based on eigenvalue analysis to assess the small signal stability of the MVAC and the MVDC architectures, along with the methods to improve the small signal stability.

CHAPTER 4

MODELING AND TRANSIENT STABILITY ANALYSIS OF VSC-MVDC SYSTEMS

4.1 Introduction

The problem with a thyristor based HVDC system is that the reactive power cannot be controlled independent of the active power. The decoupling of active and reactive power is possible with IGBT based VSC, as explained in chapter II. The independent control of active and reactive powers makes VSC-HVDC a good choice for high power DC applications. The proposed MVDC architecture [5] for the shipboard power system requires 5000 V to be maintained across the DC link, which can be achieved by controlling one VSC as DC voltage regulator. The other VSCs connected to the DC ring operate as power dispatchers which try to maintain the power at a specified reference value. This work presents the modeling and simulation of a two-terminal VSC-MVDC system and also a simplified MVDC architecture, similar to a MTDC, with two synchronous machines in MATLAB Simulink.

4.2 Control of VSC

A VSC can be controlled to achieve the following modes

- i) DC voltage control.
- ii) Active power control.
- iii) Reactive power control.
- iv) AC voltage control

The use of a particular mode of operation depends on the specific application. One or a maximum of two control modes can be used for a VSC at a time but all the modes cannot be implemented simultaneously. Some reports include literature [31] also include a frequency controller, which can be used to control the frequency, if the load is passive. In this work, for a two terminal VSC-MVDC, the first converter is assumed to operate in constant DC voltage control mode [35, 10] and the second converter acts as power dispatcher [36]. The circuit of a two-terminal VSC-HVDC can be used to explain the system. This is shown in figure 4.1.

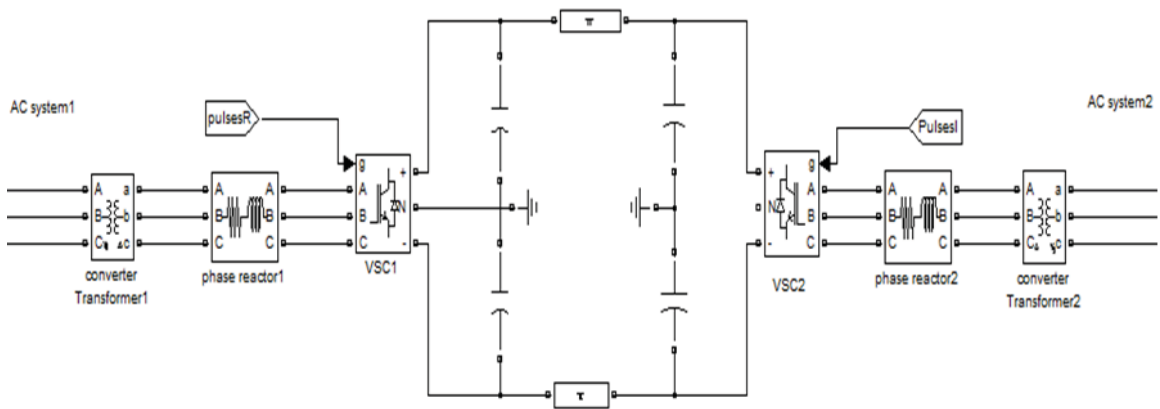


Figure 4.1 A Typical two-terminal VSC-HVDC system.

The mathematical model [10] for this system can be explained as given below.

The three phase voltages and currents can be written as

$$V_{1abcV} = R_1 i_{1abcV} + L_1 V \frac{di_{1abc}}{dt} + V_{1abc,conv} \quad (4.1)$$

where,

V_{1abc} is the voltage on the AC side of VSC1.

i_{1abc} is the AC side current of VSC1.

$V_{1abc,conv}$ is the AC side voltage of VSC1.

R_1 and L_1 are the resistance and inductance of the phase reactor connected between the AC system and the converter.

These abc quantities are converted to dq frame and rearranged to get the following form.

$$L_1 v \frac{di_{1d}}{dt} = -R_1 i_{1d} + \omega L_1 i_{1q} + V_{1d} - V_{1d,conv} \quad (4.2)$$

$$L_1 v \frac{di_{1q}}{dt} = -R_1 i_{1q} - \omega L_1 i_{1d} + V_{1q} - V_{1q,conv} \quad (4.3)$$

The above two equations can be written for the other converter with the change in subscript to 2.

The power flow equation, between the AC and DC sides, is given by

$$p_{1V} = \frac{3}{2} (v_{1d} i_{1d} + v_{1q} i_{1q}) = V_{dc1} I_{dc1} \quad (4.4)$$

where,

V_{dc1} and I_{dc1} represent the voltage and current on the DC side.

The current flowing through the DC capacitor C_1 is given by,

$$\frac{C_1 dV_{dc1}}{dt} = I_{dc1} - I_{line} \quad (4.5)$$

where,

$$I_{dc1} = \frac{P_{1V}}{V_{dc1}} \quad (4.6)$$

I_{line} is the current through the DC line

p_1 is the AC side power of VSC1

V_{dc1} is the DC voltage of VSC1

The d-axis of the rotating dq reference frame is aligned with the AC source voltage to make $v_{qv} = 0$. With this alignment, the instantaneous real and reactive power can be expressed as

$$p_{1V} = \frac{3}{2} V_{1V} (v_{1d} i_{1d}) \quad (4.7)$$

$$q_{1V} = \frac{3}{2} V_{1V} (v_{1d} i_{1q}) \quad (4.8)$$

From the above equations, it is clearly understood that the active and reactive components of the current can be used to control the active and reactive power, respectively. The two equations corresponding to the second VSC are as follows:

$$\frac{C_{2d}}{dt} \frac{dc_{2V}}{dt} = I_{lineV} - I_{dc2} \quad (4.9)$$

$$I_{dc2V} = \frac{P_{2V}}{V_{dc2V}} \quad (4.10)$$

where,

p_2 is the AC side power of VSC2.

V_{dc2} is the DC voltage of VSC2.

From equations (4.2) and (4.3), it can be seen that the two axes are coupled due to the cross terms. These two terms, $\omega L i_{1q}$ and $\omega L i_{1d}$, are made independent of each other, so that d and q-axis currents can be controlled independently.

4.2.1 Constant DC Voltage Regulator

The control structure for VSC1 operating as DC voltage regulator is shown in figure 4.2. The block diagram, shown in this figure is briefly explained. The Phase Locked Loop (PLL) block is used to get the transformation angle from abc to dq transform block. This angle is achieved by synchronization with the source voltage. The

abc to dq transform block gives the values of d, q axes currents (I_d , I_q) and voltages (V_d , V_q). The next step is to produce the reference values corresponding to these currents and voltages. These d, q axes currents and voltages are made to track the reference values. The DC voltage control block takes the DC voltage across the DC bus and compares it with the reference value to produce the error signal. This error signal is given as input to the PI controller, which produces the reference value of d-axis current (I_{dref}). The DC voltage control block acts as outer control loop. The current controller (inner current control) block takes the d, q axes currents and d, q axes reference values to produce the dq components of voltage for the converter (V_{dconv} , V_{qconv}). These values are used by the PWM generator to generate the switching signals for the VSC.

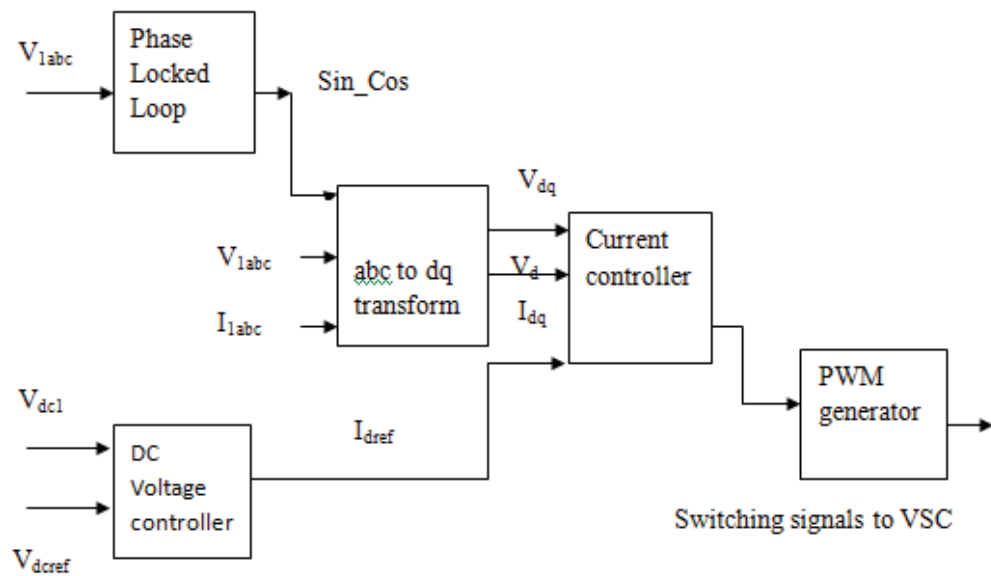


Figure 4.2 DC Voltage control diagram of VSC [10, 35].

4.2.2 Constant Power Regulator

The control schemes for active and reactive power are shown in figure 4.3. The three phase voltages and currents in the abc frame have been transformed into the rotating dq reference frame using PLL. In the active power control scheme, the reference power, P_{ref} , is compared with the calculated power, P_1 , given in equation (4.11), to get the error signal to the PI controller to generate the reference value of d-axis current. This is compared with the d-axis current, generated through dq transformation. The error between these two currents is an input to the PI controller to produce the d-axis voltage for the generation of switching signals.

$$p_{1v} = v_a i_a + v_b i_b + v_c i_c \quad (4.11)$$

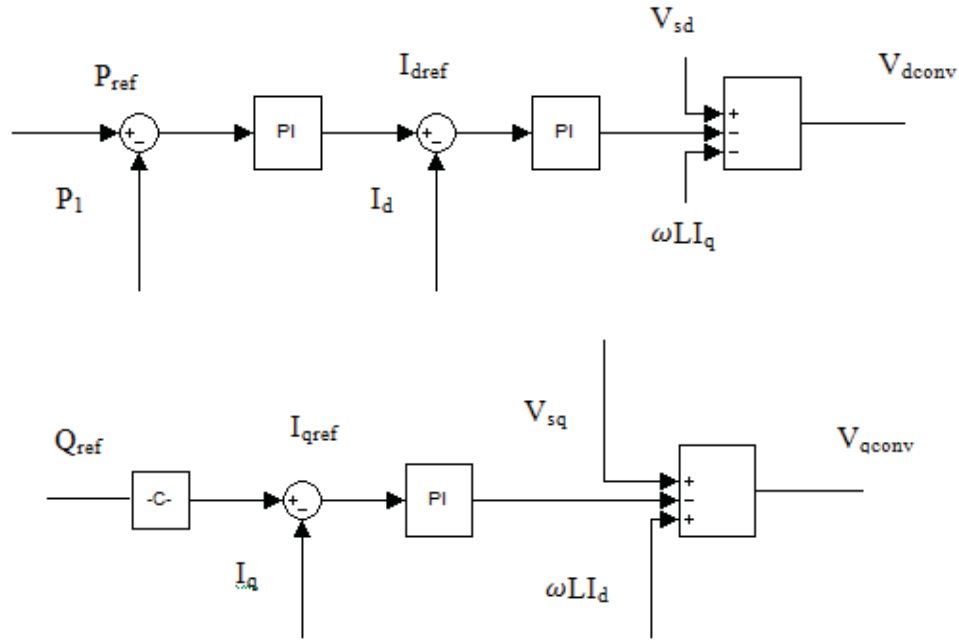


Figure 4.3 Top: Active Power Control for VSC [36]. Bottom: Reactive Power Control for VSC [36].

The reactive power scheme is also implemented in the same way as the active power control scheme. Here, instead of comparing the reference value with the calculated value of reactive power, the q-axis reference current is obtained directly from equation (4.8). It is, then, compared with the q-axis current generated from dq transformation and the error signal is fed to the PI controller to get the q-axis voltage used in the generation of switching signals.

As explained in chapter II, the relationship between the converter AC voltage and the DC link voltage is given by

$$v_{abc,conv} = \frac{2}{3} V_M \sin(\omega t + \delta) \frac{V_{dc}}{2} \quad (4.12)$$

where,

M is the modulation, the ratio between the modulation signal and the carrier signal.

δ is the angle between the fundamental voltage of the AC system and the converter AC voltage.

Correspondingly, $V_{d,conv}$ and $V_{q,conv}$ can be defined as follows

$$V_{d,conv} = \frac{2}{3} V_M \sin \delta \quad (4.13)$$

$$V_{q,conv} = \frac{2}{3} V_M \cos \delta \quad (4.14)$$

M and δ can be computed from the above two equations to get the switching signals for the VSC.

The PI controller parameters are selected based on the criteria explained in the next section. In general, the inner current loop should be at least ten times faster than the outer voltage control loop. These values are selected based on the time response obtained for a step input.

4.3 Tuning of PI Controllers

The tuning of the PI controller, used in the current controller (inner loop), is achieved through the modulus optimum condition [10], and the tuning of PI controller used in the voltage controller (outer loop) is achieved through the symmetrical optimum condition [10]. These two conditions are briefly explained below.

4.3.1 Modulus Optimum Condition

The modulus optimum condition is generally preferred because of its fast response (which is always desired for the inner loop). This method is used in tuning the controllers of lower order control systems. This method is based on simplification by pole cancellation of the system transfer function, while value of the closed loop gain is maintained at a value greater than unity. The inner current control loop in the system should have a faster response as compared to the outer loop and this is achieved with the help of the modulus optimum condition discussed in [37]. The open loop transfer function [10] corresponding to PI current control scheme is given by the following expression:

$$G_{1V} = K_{p1V} \left(\frac{1+T_{i1}s}{T_{i1}sV} \right) \cdot \frac{1V}{1+T_a s} \cdot \frac{1}{R} \frac{1}{1+s\tau_{1V}} \quad (4.15)$$

where,

$K_{p1V} \left(\frac{1+T_{i1}s}{T_{i1}sV} \right)$ is the transfer function of the PI controller.

$\frac{1}{1+T_a s}$ is the transfer function of PWM converter.

$\frac{1}{R} \frac{1}{1+s\tau}$ is the system transfer function.

K_{p1} and T_{i1} are the parameters of the PI controller.

$T_{av} = \frac{1}{2 \cdot \text{switching frequency}}$ is the delay introduced by VSC switches.

τ_1 is the time constant of the line.

The time response of this transfer function to step input is studied and correspondingly the values of gain and integral constants of the PI controller are found.

4.3.2 Symmetrical Optimum Condition

Tuning of the PI controller, using modulus optimum criteria, is possible when the controlled system has one major time constant and other negligible time constants. When the transfer function of the system has one pole at the origin, the pole shift does not help in maintaining the desired system response and modulus optimum condition is not preferred in such cases. The symmetrical optimum condition tries to maximize the phase margin of the system for a given frequency so that the system can withstand more delays. This property is desirable for the outer loop which should act slowly compared to the inner loop.

The open loop transfer function [10] for the voltage regulator

$$G_{2V} = K_{p2} \left(\frac{1+T_{i2}s}{T_{i2}sV} \right) \cdot \frac{1V}{1+T_{eq}s} \cdot \frac{d}{dcv} \frac{\omega C}{s} \quad (4.16)$$

where,

$K_{p2} \left(\frac{1+T_{i2}s}{T_{i2}sV} \right)$ is the transfer function of the PI controller.

$\frac{1}{1+T_{eq}s}$ is the transfer function of the approximated current controller.

$\frac{dV\omega CV}{dcv s}$ is the transfer function corresponding to the DC link dynamics.

K_{p2} and T_{i2} are the parameters of the PI controller used in the outer loop.

T_{eq} is the time constant of the approximated first order current control loop.

The Bode plot of the open loop transfer function gives the stable operating limits with a maximum phase margin. The time response of this transfer function to a step input is studied and correspondingly the values of gain and integral constants of the PI controller are found. Using these two conditions, the PI controllers, in the inner current control loop and outer voltage control loop are tuned to make the steady state error zero.

4.4 Two-Terminal VSC-MVDC

A two-terminal VSC-MVDC system was first implemented to look at the behavior of the above discussed controllers, i.e. DC voltage regulator and the power dispatcher. The two terminal VSC-MVDC system is shown in figure 4.4.

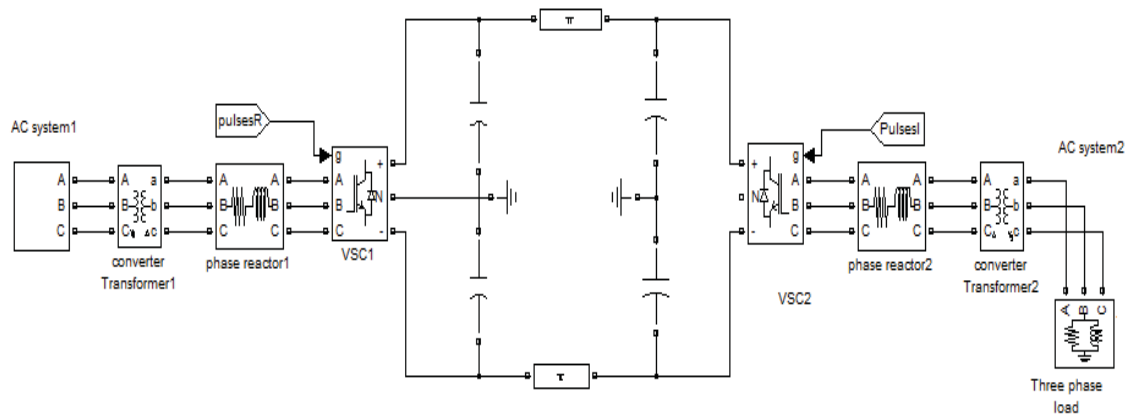


Figure 4.4 A Two-terminal VSC-MVDC system.

In this figure, VSC1 acts as DC voltage regulator and VSC2 acts as power dispatcher. VSC1 is connected to a synchronous machine of 36 MVA, 4.16 kV, 60 Hz rating (AC system1) through the converter transformer and the phase reactor. The synchronous machine is assumed to be provided with a steam turbine governor (The

actual shipboard power system employs a gas turbine, but due to the lack of this in Simulink library, a steam turbine has been used for this work) and excitation system. The voltage of the secondary winding of the transformer depends on the DC voltage to be maintained across the DC bus. This is explained in equation (4.12). Correspondingly the values of the secondary voltage of the transformer and the phase reactor values are selected. In this case, to maintain 5000 V across the DC bus, the value of the secondary voltage of the transformer is found to be at least 3.16 kV. The same configuration is seen for VSC2, which is controlled as a ‘Power dispatcher’. A load of 12 MVA is connected at the other end. The voltages on either end of the DC link are shown in figure 4.5.

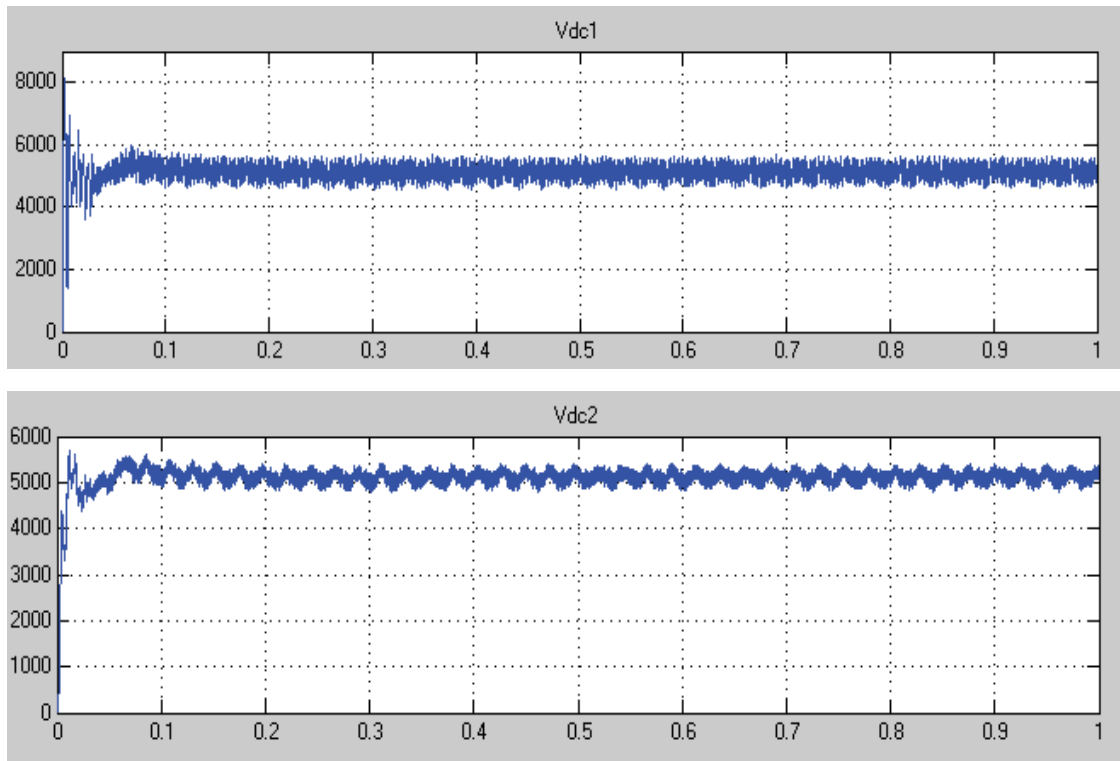


Figure 4.5 Top: Voltage across the DC link (rectifier end). Bottom: Voltage across the DC link (inverter end).

The first waveform corresponds to the DC voltage across the capacitor terminals of VSC1 (V_{dc1}). This is maintained at 5000 V with the help of the voltage regulator and the second waveform represents the voltage across the capacitor terminals of VSC2 (V_{dc2}) i.e. the DC voltage after the DC link.

$$V_{dc1V} = V_{dc2V} + \text{drop across DC lineV}$$

In this study, the length of the DC link is assumed to be 1 km. The 1 km length is selected to look at the drop across the DC link. The resistance of the line [49] being small (taken as 0.0007 ohm/km), the drop across the line is negligible and the same 5000 V are applied across the terminals of VSC2. Power is maintained at the reference value through the power dispatcher mode of VSC2 and the voltage across the load is represented in figure 4.6. The voltage shown in the figure is close to 5880 V which is the peak value of the 4.16 kV AC system 2. After implementing two-terminal VSC-MVDC, the next step was to extend it to a multi-terminal VSC-MVDC system.

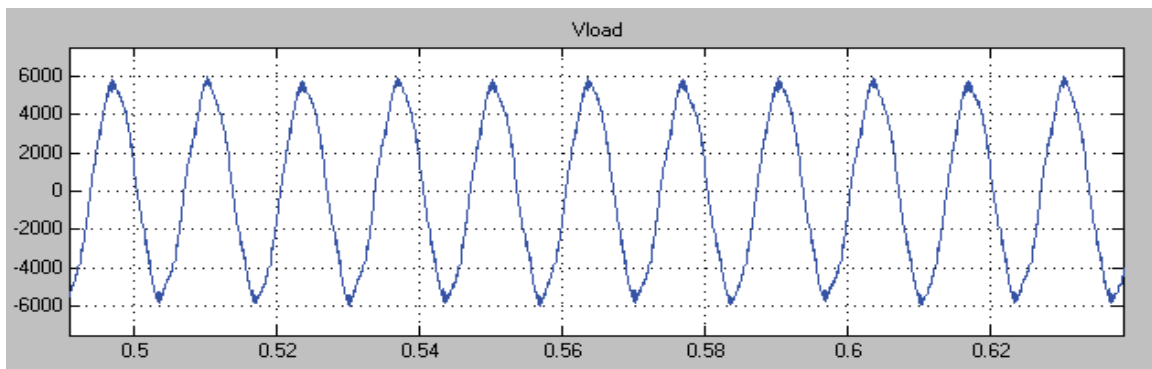


Figure 4.6 Load voltage for two-terminal VSC-MVDC.

4.5 Multi-Terminal DC Ring Structure

MTDC is an extended concept of the two-terminal VSC-MVDC. The MTDC ring structure, simulated in this work, is shown in figure 4.7. This represents a simplified diagram of the shipboard power system with two synchronous generators connected to the DC ring structure.

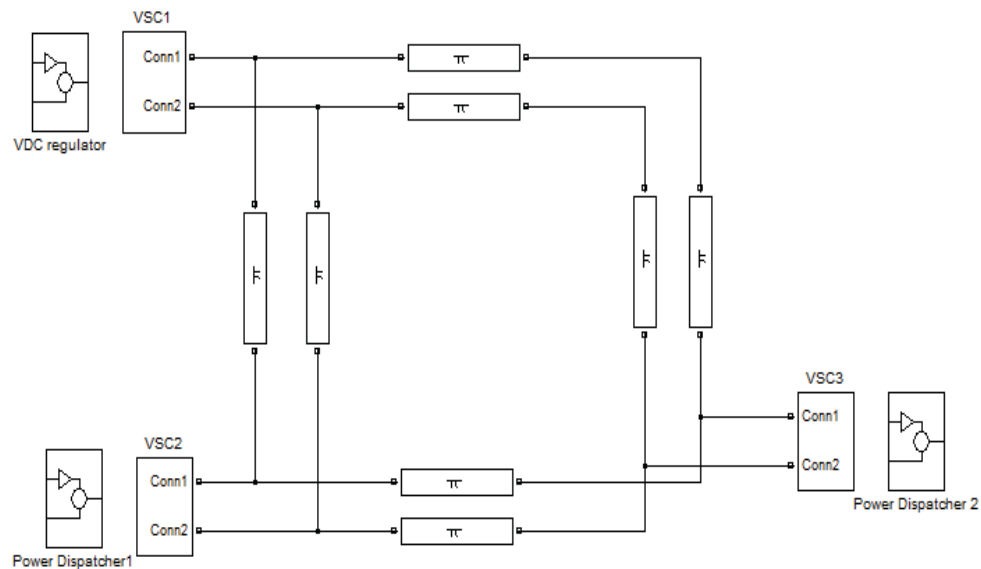


Figure 4.7 A Multi-Terminal Ring Structure of MVDC system.

In this structure, VSC1 acts as DC voltage regulator and controls the DC voltage across the bus. VSC2 and VSC3 act as power dispatchers. All the pi sections of lines forming the DC ring structure are assumed of 1 km length. The subsystem representing the VSC in this figure consists of the synchronous machine, converter transformer and the phase reactor. The internal diagram of the VSC1 subsystem is shown in figure 4.8. The internal representation of the voltage regulator and the power dispatcher are shown earlier in figures 4.2 and 4.3 respectively.

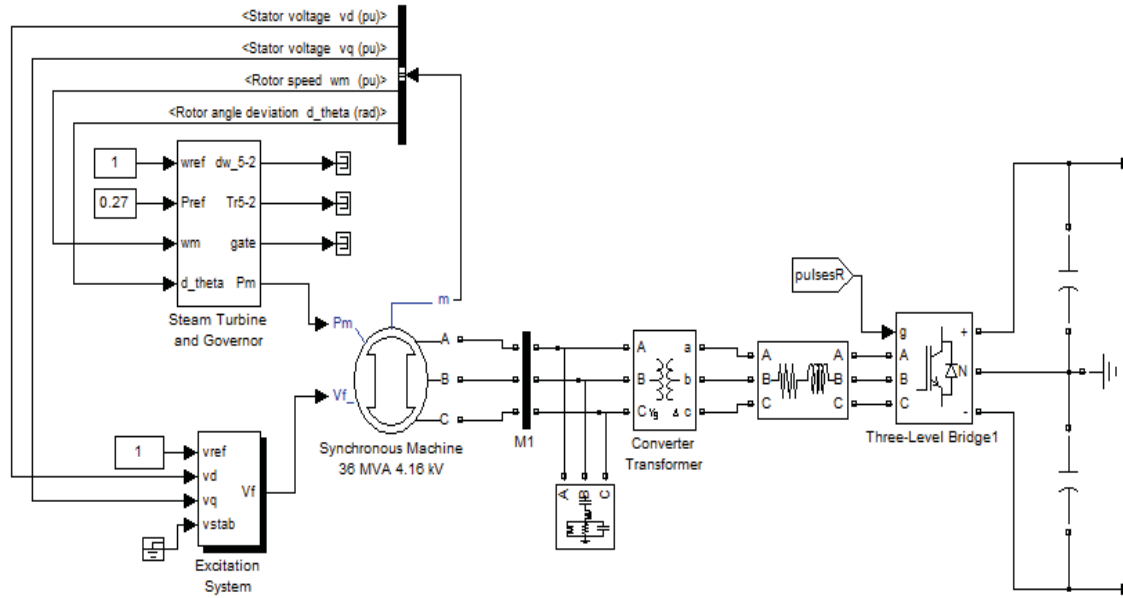


Figure 4.8 VSC1 Subsystem MATLAB Simulink diagram.

The desired voltage of 5000 V across the DC bus is maintained with the help of voltage regulator. Vdc1 represents the voltage on the rectifier end in one part of the DC ring. The voltage regulator tries to regulate the voltage at 5000 V but the distortion is more compared to the two-terminal VSC-MVDC system. The length of the DC link is the same as the previous case and Vdc2 exhibits similar pattern with undesirable distortion voltages. This is measured at the other end of the DC link. The voltages on either ends of the DC link in one part of the ring structure are shown in figure 4.9.

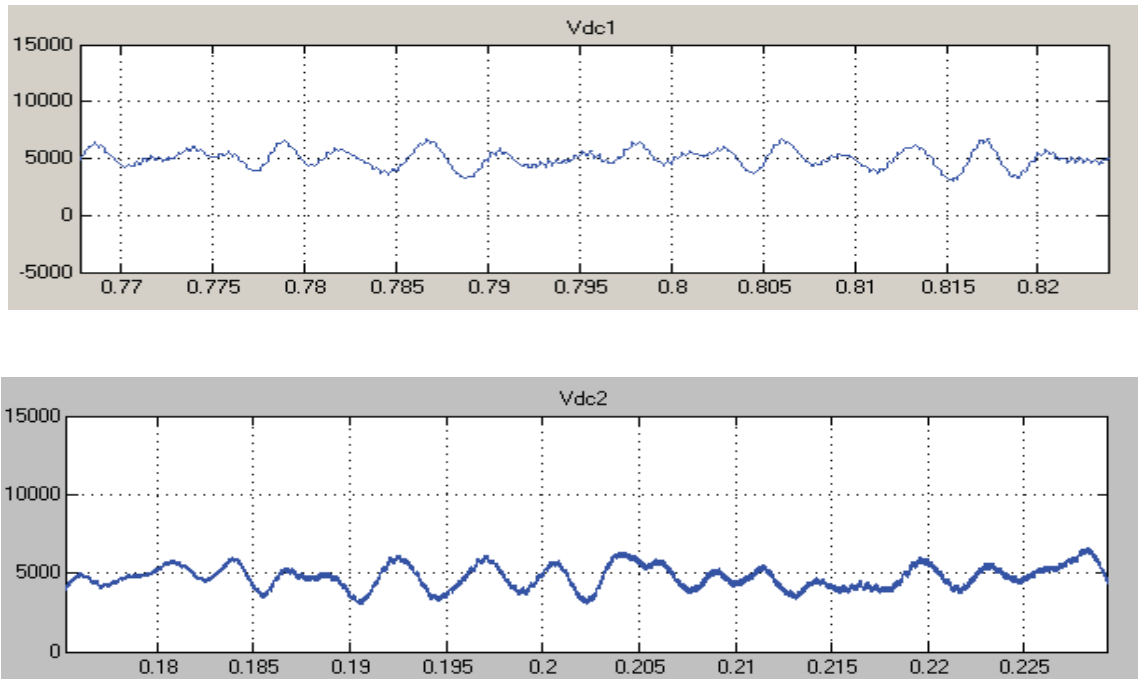


Figure 4.9 Top: Voltage across the DC link (rectifier end) for the MTDC system. Bottom: Voltage across the DC link (inverter end) for the MTDC system.

The load is also shared between the two generators. The reference mechanical power to the governor is given based on the value of load it has to supply. The reference values of the active and reactive power are set based on the active and reactive load connected to the system. The voltage across the load is plotted in figure 4.10.

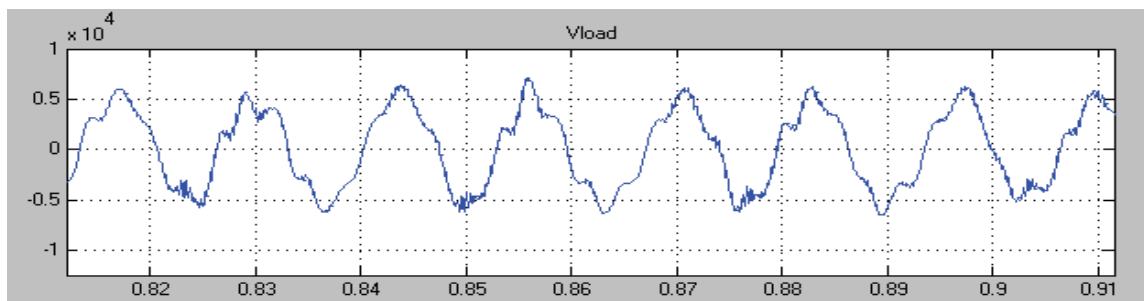


Figure 4.10 Load voltage for the MTDC System.

The voltages across the load are also more distorted compared to the two-terminal VSC-MVDC system. This can be attributed to the need of better filtering elements. Additional filtering will be part of the future work.

4.6 Transient Stability Analysis for MTDC Ring Structure

Transient stability studies are also conducted on the MTDC ring structure, explained above. The rotor angle deviation under normal conditions is shown in figure 4.11.

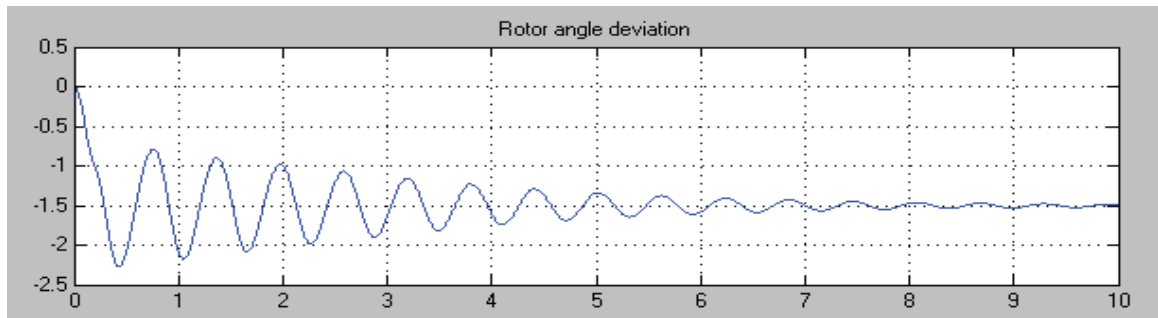


Figure 4.11 Rotor angle deviation of Synchronous machine 2.

A three phase fault is applied at the synchronous generator 2 terminals to look at the transient behavior of the system. The fault is applied at 0.1 sec for duration of 0.05 sec. The system becomes unstable and this can be explained by looking at the rotor angle deviation of the generator 2 shown in figure 4.12.

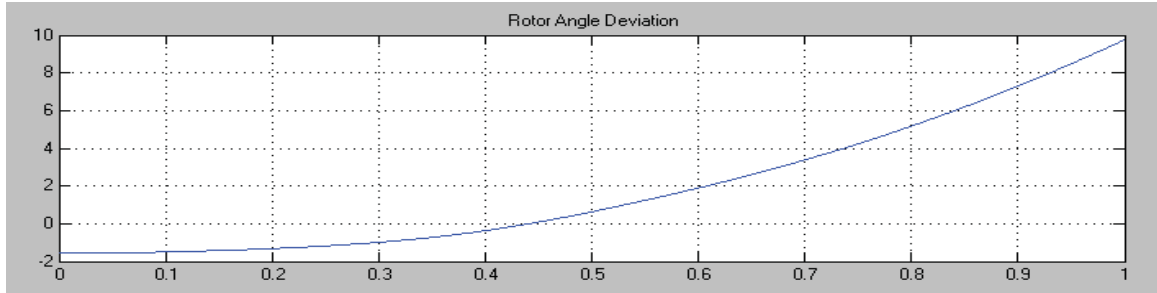


Figure 4.12 Rotor angle deviation of Synchronous machine 2 (fault applied).

The rotor angle deviation goes on increasing after the fault is applied and eventually the system becomes unstable. One assumption made here is that the fault does not occur at VSC1, i.e. the voltage regulator is assumed to maintain constant DC voltage all the time.

4.7 Summary

This chapter provides descriptions about the available control modes of a VSC. The DC voltage control, active power control, and reactive power control modes are explained and implemented for a two-terminal VSC-MVDC system. The tuning of PI controller parameters using Modulus Optimum and Symmetrical Optimum conditions are described. The two-terminal VSC-MVDC system concepts are extended to a MTDC architecture forming a DC ring structure. The behavior of the system following a 3-phase fault is also observed for the system transient stability

CHAPTER 5

SMALL SIGNAL STABILITY ANALYSIS OF SHIPBOARD POWER SYSTEMS

5.1 Introduction

Power system stability can be defined [33] as the ability of a power system to maintain synchronism under normal operating conditions and to regain an acceptable state of equilibrium after being subjected to a disturbance. In general, stability can be described as the equilibrium between opposing forces. In case of interconnected synchronous machines, this equilibrium is maintained with the help of restoring forces, which try to accelerate or decelerate one or more machines with respect to the others. Under a steady state condition, the speed remains constant if the input mechanical torque becomes equal to the output electrical torque of each synchronous machine. This equilibrium is disturbed, when the system is perturbed. When a synchronous machine loses synchronism, the angular separation(δ) between the rotors of the two machines increases and the faster machine picks most of the load. This can be explained with the help of its simplified power-angle relationship, given by the following expression [33]. The power transfer in a two machine system is shown in figure 5.1 and the idealized model for a two machine system is shown in figure 5.2.

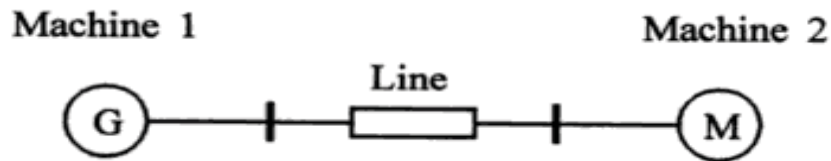


Figure 5.1 Power transfer in a two machine system [33].

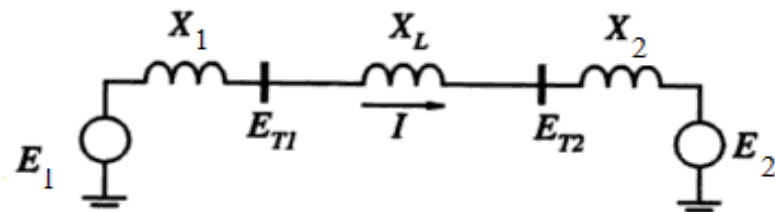


Figure 5.2 Idealized model for a two machine system [33].

$$P = \frac{E_1 E_2 \sin \delta}{X_{TV}} \quad (5.1)$$

$$X_{TV} = X_{1V} + X_{LV} + X_2 \quad (5.2)$$

where,

P is the power transferred from machine 1 to machine 2.

δ is the angular separation between the rotors of the two machines.

X_T is the total transfer reactance between internal voltages of the two machines.

E_1, E_2 are the internal voltages of the two machines.

Beyond a particular value of (δ), the power- angle relationship is no longer valid and the system becomes unstable. The stability of the interconnected power system depends on sufficient restoring torques (forces), which are produced by variations in rotor angle. Following a perturbation, the equation describing the electrical torque of a synchronous machine varies and this can be expressed as the sum of two components: i) the first is the

torque component in phase with the rotor angle perturbation, and ii) the second is the torque component in phase with the speed deviation.

$$\Delta T_{eV} = T_s \Delta \delta + T_D \Delta \omega \quad (5.3)$$

where,

ΔT_e is the change in electrical torque

$T_s \Delta \delta$ is the synchronizing torque component

$\Delta \delta$ is the rotor angle perturbation

$T_D \Delta \omega$ is the damping torque coefficient

$\Delta \omega$ is the speed deviation

Both of these torque components are important in maintaining system stability. Insufficient synchronizing torque may result in large variation in the rotor angle leading to instability, and lack of sufficient damping torque may result in oscillatory instability. Based on these facts, the rotor angle stability phenomenon is characterized into the following categories:

1. Small signal stability
2. Transient stability

Small signal stability is the ability of the power system to maintain synchronism under small disturbances, which are always present in any interconnected power system. These small disturbances are due to load and generation changes. So the dynamic equations describing the system can be linearized for the purpose of small signal stability analysis. Small signal instability can be of the form:

- i) Insufficient synchronizing torque leading to a steady increase in rotor angle.

- ii) Insufficient damping torque leading to rotor oscillations of increasing amplitude.

Small signal stability problems can be explained simply as insufficient damping of oscillations. Some important unstable modes [33] are as briefly explained.

- i. Local modes: These oscillations are confined to at a small region of the power system and, hence, the name local modes. These are characterized with the swinging of units at one generating station against the rest of the power system.
- ii. Inter-area modes: These oscillations are observed between groups of machines in different areas (regions) connected through weak tie-line.
- iii. Control modes: These oscillations are due to poorly tuned exciters, HVDC converters, speed governors, and static VAR compensators and are, generally, associated with generator units and their controls.
- iv. Torsional modes: These oscillations are due to the interaction with excitation controls, speed governors, HVDC controls, and series-capacitor compensated lines and are, generally, attributed to turbine-generator shaft system.

This chapter has mainly focused on detailed analysis of rotor angular stability of the system, specifically the small signal stability. A linearized dynamical model of the power system around an initial operating point has been used to analyze the small signal stability of MVAC and MVDC architectures of the zonal shipboard power systems. Results obtained at a base operating point, through AC-DC load flow, have been used as the initial operating point for linearizing the system equations. Eigenvalue analysis of the system state matrix has been carried out to assess the small signal stability of the systems.

5.2 Methodology for Small Signal Stability

The small signal stability of an AC system refers to its ability to maintain synchronism, when subjected to a small disturbance. These small disturbances are inherent in the system due to small changes in loads and generation. It utilizes linearized analysis of the dynamical system around an equilibrium operating point, as described below.

The mathematical equations [33, 38] governing any dynamical system can be represented in state space form as.

$$\dot{\mathbf{X}} = \mathbf{f}(\mathbf{X}, \mathbf{U}) \quad (5.4)$$

along with output equations

$$\mathbf{Y} = \mathbf{g}(\mathbf{X}, \mathbf{U}) \quad (5.5)$$

where,

\mathbf{X} is the state variables vector

\mathbf{Y} is the output variables vector, and

\mathbf{U} is the control variables vector

At equilibrium or singular point, the derivatives of the state variables are zero.

$$\dot{\mathbf{X}} = \mathbf{f}(\mathbf{X}_0) = \mathbf{0}$$

where,

\mathbf{X}_0 represents the state vector \mathbf{X} at equilibrium point.

Any small perturbation disturbs the natural balance in the system, resulting in changes in variables such as $\Delta\mathbf{X}$, $\Delta\mathbf{Y}$, and $\Delta\mathbf{U}$. Now the system equations can be written in linearized form as,

$$\Delta \dot{\mathbf{X}} = \mathbf{A} \Delta \mathbf{X} + \mathbf{C} \Delta \mathbf{U} \quad (5.6)$$

$$\Delta \mathbf{Y} = \mathbf{O} \Delta \mathbf{X} + \mathbf{F} \Delta \mathbf{U} \quad (5.7)$$

\mathbf{A} is the state or plant matrix.

\mathbf{C} is the control or input matrix.

\mathbf{O} is the output matrix.

\mathbf{F} is the feed-forward matrix.

where,

The elements of these matrices are defined as

$$\mathbf{A} = \left[\frac{\partial \mathbf{f}}{\partial \mathbf{X}} \right], \mathbf{C} = \left[\frac{\partial \mathbf{f}}{\partial \mathbf{U}} \right], \mathbf{O} = \left[\frac{\partial \mathbf{g}}{\partial \mathbf{X}} \right] \text{ and } \mathbf{F} = \left[\frac{\partial \mathbf{g}}{\partial \mathbf{U}} \right]$$

All the derivatives are calculated at the initial equilibrium operating point. In the power system network, the initial operating point can be obtained through load flow solution at given base operating point.

It can be shown that the closed loop poles of the above system are the roots of the characteristic equation,

$$\det (\mathbf{s I} - \mathbf{A}) = 0 \quad (5.8)$$

The roots of the above equation give the eigenvalues of the state matrix \mathbf{A} .

The eigenvalues $\boldsymbol{\lambda} = (\lambda_1, \lambda_2, \dots, \lambda_n)^T$ of the state matrix \mathbf{A} , of size $n \times n$, can be obtained by finding the roots of the characteristic equation

$$\det (\mathbf{A} - \boldsymbol{\lambda} \mathbf{I}) = 0 \quad (5.9)$$

By looking at the eigenvalues $\lambda_i = \alpha_i \pm j\omega_i$, which are given by the roots of the characteristic equation of the system state matrix \mathbf{A} , the following conclusions [48] on small-signal stability can be made,

1. The system is stable if all the eigenvalues lie in the left half of the complex plane.
2. The system is unstable if at least one eigenvalue lies in the right half of the complex plane (or if one or more eigenvalues lie on the imaginary axis).
3. The system is marginally stable if the eigenvalue lies on the imaginary axis

Associated with each eigenvalue, there are two eigenvectors known as 'right eigenvector' and 'left eigenvector'. Right Eigenvector (REV) Φ_i , corresponding to eigenvalue λ_i satisfies the condition: $\mathbf{A}\Phi_i = \lambda_i \Phi_i$

REV matrix Φ is defined as $\Phi = [\Phi_1, \Phi_2, \dots, \Phi_n]$

Left eigenvector (LEV) Φ_i , corresponding to eigenvalue λ_i satisfies the condition:

$$\Phi_i \mathbf{A} = \Phi_i \lambda_i$$

LEV matrix Φ is defined as $\Phi = [\Phi_1, \Phi_2, \dots, \Phi_n]^T$

The above matrices are orthogonal matrices and are said to be in normalized form, if $\Phi \Phi^T = \mathbf{I}$ (identity matrix).

Participation matrix combines the right and left eigenvectors to relate the system state variables and the modes. Participation factors, P_{ki} (k th element of the state participation matrix \mathbf{P}), can be determined utilizing elements of the normalized LEV and REV matrices, as,

$$\mathbf{P} = [\mathbf{P}_1, \mathbf{P}_2, \dots, \mathbf{P}_n]$$

$$P_{ki} = \Phi_{ki} \cdot \rho_{ik} \quad (5.10)$$

where,

Φ_{ki} represents the ki^{th} element of the REV matrix (k-th entry of REV Φ_i).

ρ_{ik} represents the ik^{th} element of the LEV matrix (k-th entry of LEV ρ_i).

Participation factor P_{ki} , determines the relative participation of the k^{th} state variable (x_k) in the i^{th} mode of oscillation (λ_i) and it is dimensionless. Under poor damping of the system, the state having maximum participation to the critical mode can be selected to design the proper controller.

The small signal stability analysis has been performed in this work with the help of a Power System Toolbox (PST) [34]. PST was developed by Cherry Tree Scientific Software Company, Canada to carry out power system analysis within MATLAB®. The differential equations representing the power system component models were written in MATLAB m-files to perform load flow, voltage stability, transient stability, small signal stability and participation analysis. These m-files have models for synchronous generators, exciters, governors, power system stabilizers, induction motor loads and lumped loads. In PST, the linearization is performed by calculating the Jacobian matrix numerically and there is some loss of accuracy, particularly in the zero eigenvalue which is characteristic of most inter-connected power systems. The tool box builds the state matrix using a perturbation model.

5.3 Power System Component Models

In the present study, the following models of various power system components have been used. The parameters of these components were given as an input file to PST.

5.3.1 Synchronous Generator

A two-axis sub transient model [38-40] has been utilized in this work. The equations governing the dynamics of an i^{th} synchronous generator can be written as:

$$\dot{\delta} = \omega_i - \omega_s \quad (5.11)$$

$$\dot{\omega}_i = \frac{1}{2H_i} \left[P_m - [E_{qi} - X_{di} I_{di}] I_{qi} - [E_{di} - X_{qi} I_{qi}] I_{di} - D_i (\omega_i - \omega_s) \right] \quad (5.12)$$

$$\dot{E}_{qi} = \frac{1}{T_{doi}} \left[-E_{qi} - (X_{di} - X_{di}) * I_{di} + E_{fdi} \right] \quad (5.13)$$

$$\dot{E}_{di} = \frac{1}{T_{qoi}} \left[-E_{di} - (X_{qi} - X_{qi}) * I_{qi} \right] \quad (5.14)$$

$$\dot{E}_{di} = \frac{1}{T_{qoi}} \left[-E_{di} - (X_{qi} - X_{qi}) * I_{qi} \right] \quad (5.15)$$

$$\dot{E}_{qi} - E_{qi} = \frac{1}{\left[\frac{(X_{di} - X_{di}) k_5 E_q}{(X_{di} - k_6 X_{al}) V} - (E_{qv} - E_q) \right]} V \quad (5.16)$$

where,

δ_i is rotor angle.

ω_i is the rotor speed.

ω_s is the synchronous speed.

E_{fdi} is the field voltage.

H_i is the inertia constant.

D_i is the damping coefficient.

P_m is the mechanical input power.

E_{di} and E_{qi} are the induced voltages in the d and q axes.

I_{di} and I_{qi} are the stator currents in the d and q axes.

X_{al} is the armature leakage reactance.

X_{di} and X_{qi} are the reactances in the d and q axes.

X'_{di} and X'_{qi} are the transient reactances in the d and q axes.

X''_{di} and X''_{qi} are the sub-transient reactances in the d and q axes.

T'_{doi} and T'_{qoi} are the transient time constants in the d and q axes.

T''_{doi} and T''_{qoi} are the sub-transient time constant in the d and q axes.

k_5, k_6 are the machine constants [41].

5.3.2 Exciter

5.3.2.1 IEEE Type-0

A simple IEEE Type-0 exciter model [33, 42] has been considered along with each synchronous generator. This model takes a reference voltage and the generator terminal voltage as inputs, and provides an excitation voltage to the synchronous machine. Type-1 exciter [42] has also been considered to look at the damping of the system. The equations corresponding to the exciter model are:

$$\dot{V}_r = \frac{1}{T} [V_{TV} - V_r] \quad (5.17)$$

$$\dot{E}_{fd} = \frac{1}{T_{AV}} [K_A (V_{ref} - V_t) - E_{fd}] \quad (5.18)$$

where,

K_A is the amplifier gain.

T_A is the amplifier time constant.

V_{ref} is the reference voltage.

V_T is the terminal voltage.

E_{fd} is the field voltage.

5.3.3 Propulsion motor load

A double cage induction motor model has been used in this work to represents the naval shipboard system propulsion motor load. The equations governing its dynamics [43] are:

$$E_{qmi} \dot{V} = \frac{\left[\frac{X_i}{X_i} E_{qmi} + \left(\frac{X_i - X_i}{X_{iV}} \right) V_i + T_{moi} (w_{mi} - w_s) E_{dmi} \right]}{T_{moiV}} V \quad (5.19)$$

$$E_{dmi} \dot{V} = \frac{\left[\frac{X_i}{X_i} E_{dmi} - T_{moi} (w_{mi} - w_s) E_{qmi} \right]}{T_{moiV}} \quad (5.20)$$

$$w_{mi} \dot{M} = \frac{\left[\frac{V_i E_{dmi} - T_{mi}}{X_i} \right]}{M_{miV}} \quad (5.21)$$

where,

M_{mi} is the inertia constant.

w_{mi} is the rotor speed.

V_i is the terminal voltage.

T_{moi} is the time constant of the motor.

E_{dmi} and E_{qmi} are the transient voltages in d and q axes respectively.

5.3.4 VSC Models

This part of the work has considered a simplified steady state model [44] of the voltage source converters, utilized in the MVDC architecture. The AC sides of the converters have been represented by a voltage source connected to the AC bus through its transformer impedance. On the DC side, one of the converters (fed from MTG-1 rectifier in this study) has been assumed to operate in voltage control mode, which controls the DC voltage across the DC link and the other converters are assumed to act as power dispatchers, operating in the power control mode.

5.4 Results

For the shipboard power system with MVAC and MVDC architectures, shown in figures 2.2 and 2.3 in chapter II, the initial operating conditions were obtained from the base load flow solution developed for AC systems as well as AC-DC systems utilizing the Newton Raphson load flow method. For solving the MVDC system load flow, a sequential DC-AC approach was used in which the DC system was solved first, followed by load flow solution of the AC system. Among the two propulsion motors, only one motor PM-1 load of 36.5 MW was considered in this work. The radar and other loads were taken as a 5 MW total lumped load for the simulation purpose. The generators were assumed to share the loads according to their ratings for the base case simulation. The small signal stability analysis was carried out with the help of PST tool box considering the detailed dynamic model of generators, exciter and the induction motor driving the propulsion load.

Both the MVAC and MVDC architectures of the zonal shipboard power systems were compared to look at the small signal stability. The eigenvalues for the MVAC architecture with Type-0 exciter are plotted in figure 5.3 to analyze the small signal stability of the system.

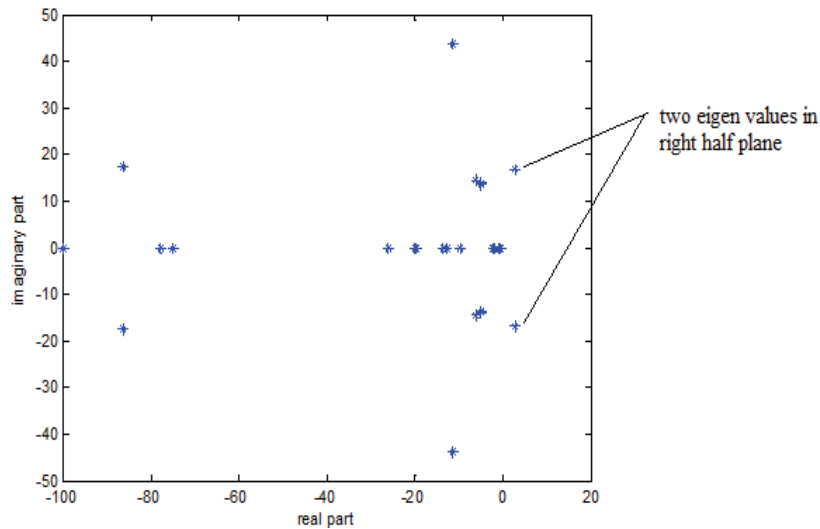


Figure 5.3 Eigenvalues for MVAC architecture with Type-0 exciter.

From this figure, it can be observed that the two eigenvalues ($2.728 \pm 16.855i$) are located on the right half of the complex plane, which make the system unstable. The damping ratio corresponding to this eigenvalue is -0.016. The damping of the system should be positive for the system to be stable. The PST toolbox specifies the minimum value of damping as 0.05 and any system with damping ratio less than this value is treated as unstable. A few other critical eigenvalues for the MVAC architecture with relatively low values of damping (exhibiting unstable mode or closer to the imaginary axis) are listed in Table 5.1 for all the case studies.

Next the eigenvalues for the MVDC architecture were obtained. The eigenvalues obtained for the MVDC architecture with Type-0 exciter are plotted in figure 5.4. All the eigenvalues have negative real parts with some of these forming complex conjugate pairs and lying on the left half of the complex plane. Thus, the MVDC system is stable. The critical damping ratio in this case is 0.0690, which is above the minimum acceptable damping ratio.

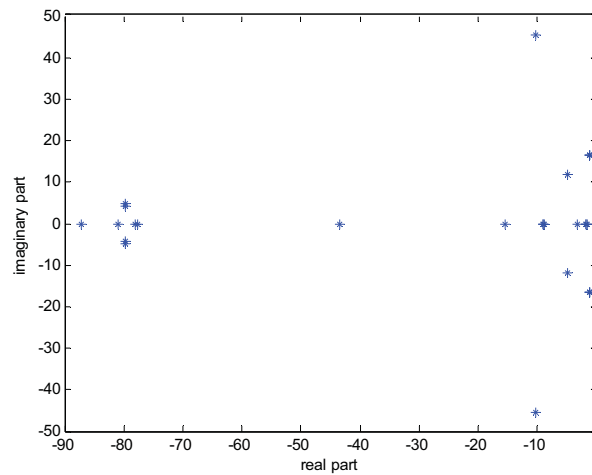


Figure 5.4 Eigenvalues for MVDC architecture with Type-0 exciter.

Some of the eigenvalues and the corresponding damping ratios for the MVAC and MVDC architectures are listed in Table 5.1. The small signal instability in MVAC architecture and the modes responsible for it can be explained with the help of participation analysis. Methods to improve small signal stability using higher order exciter (Type-1), placement of a SVC and addition of a Power System Stabilizer will be presented in chapter VI.

Table 5.1 Critical eigenvalues related to MVAC and MVDC systems with Type-0 exciters

MVAC system with Type-0 exciter		MVDC system with Type-0 exciter	
Eigenvalue	Damping ratio	Eigenvalue	Damping ratio
$2.728 \pm 16.855i$	-0.1600	$-1.158 \pm 16.44i$	0.0690
$-11.449 \pm 45.80i$	0.2529	$-1.154 \pm 16.65i$	0.0691
$-4.955 \pm 15.91i$	0.5554	$-1.201 \pm 16.55i$	0.0724
$-4.990 \pm 15.72i$	0.5417	$-10.564 \pm 45.54i$	0.2228
$-6.014 \pm 14.40i$	0.5855	$-4.891 \pm 11.89i$	0.5804

5.5 Summary

This chapter has presented the detailed explanation of eigenvalue analysis to assess the small signal stability of MVAC as well as MVDC architectures of the zonal shipboard power systems. The dynamic equations representing the detailed model of the power system components have been described. Linearized dynamical analysis has been carried out to find the eigenvalues of the state matrix. These eigenvalues were plotted in the complex plane to comment on the small signal stability of the system. From the eigenvalues obtained for Type-0 exciter, it was clear that the MVAC system is unstable and the MVDC system is stable. Small signal stability enhancement techniques for the shipboard power system with both architectures will be explained in chapter VI.

CHAPTER 6

SMALL SIGNAL STABILITY ANALYSIS ENHANCEMENT

6.1 Introduction

The reason for small signal instability in the case of MVAC architecture with Type-0 exciter can be investigated with the help of state participation analysis. From the results of the participation analysis, which identifies the state participating maximum to the critical mode, necessary control action can be initiated to improve the small signal stability. The control/corrective actions are entirely dependent on the participation factors. All the values of the critical modes contributing to instability can be arranged in a particular order based on the severity. Participation factors for the MVAC architecture are arranged in the descending order of significance and the impact of SVC, Type-1 exciter and PSS will be presented in this chapter.

6.2 Participation Analysis

As explained in chapter V, the Participation matrix helps in identifying the relationship between the states and the modes, which is derived using both the left and right eigenvectors corresponding to a critical mode. Equation (5.10), in chapter V, represents the participation factor, the (k,i) element is a measure of the relative participation of the k^{th} state variable in the i^{th} mode. Lack of dimensions also adds to the advantages of a participation factor. Participation analysis was carried out to look at the participation of states to the modes leading to instability of the MVAC architecture with

Type-0 exciter. These are shown in Table 6.1. These values are arranged in descending order, based on the relative contribution of states to the unstable mode.

Table 6.1 State participation factor to critical mode for the MVAC system with Type-0 exciter

State	Participation factor
E_q of generator 1	1.0000
E_q of generator 2	0.9580
E_{fd} of exciter 1	0.6541
E_{fd} of exciter 2	0.6151
E_{dmi} of motor	0.5971
E_{di} of generator 1	0.5512
E_{di} of generator 2	0.4919

It is observed that the generator internal voltages, exciter voltage states and induction motor voltage state are participating maximum to the unstable mode. Since the instability is due to lack of providing effective voltage control, the impact of placing an SVC at the load bus was studied on the small signal stability of the system.

6.3 Static VAR Compensator (SVC)

Power system stabilizers are not effective for damping oscillations in systems having slow exciters. In such systems, electronic damping control may serve as an alternative to provide sufficient damping to the unstable modes. Electronic system controls or Flexible AC Transmission Systems (FACTS) are thyristor based system elements, which include SVCs and Thyristor Controlled Series Capacitors (TCSCs). The block diagram representation of a SVC is shown in figure 6.1.

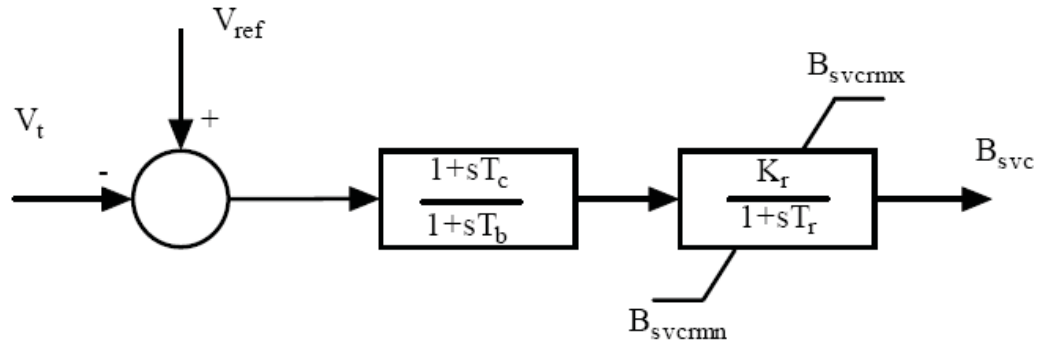


Figure 6.1 Block diagram of a SVC [45].

where,

V_{ref} is the reference voltage.

V_t is the terminal voltage.

T_b, T_c are the compensator time constants.

K_r is the regulator gain.

T_r regulator time constant.

B_{max} and B_{min} are the maximum and minimum value of susceptance.

A SVC can be used to provide voltage support at a network bus and TCSC can be used to control the flow in the transmission line. In this work, an SVC is added to improve the damping of the system. A TCSC would not benefit this study and is not explained further. The term static is used to indicate that SVCs have no rotating parts, like synchronous machines. The bus voltage support or control using a SVC is achieved by varying the shunt capacitance or reactance.

The eigenvalues obtained after placing an SVC of 20 MVAR capacity are plotted in Figure 6.2. The value of 20 MVAR is dependent on the loading of the system. In this case, the system is first provided with 10 MVAR support and the damping is recorded.

The damping ratio is not significant and it can be understood that more reactive power support is required at the load bus. Hence a SVC of 20 MVAR is added and the critical damping ratio is once again observed and represented in table 6.2

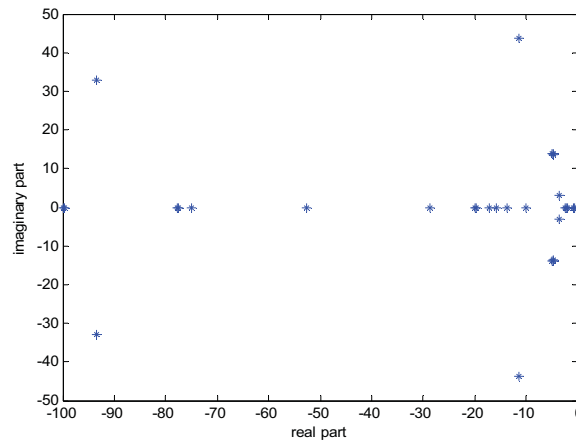


Figure 6.2 Eigenvalues for MVAC architecture with Type-0 exciter and SVC [20]MVAR] at load bus.

It can be observed from this figure that all the eigenvalues have negative real part and are located on the left half of the complex plane and, thus, the MVAC system becomes stable. The critical mode in this case has a damping ratio of 0.2529, as listed in Table 6.2 There has been a significant improvement in damping ratio from -0.016 to 0.2529 with the placement of the SVC. The placement of the SVC at other buses also improved the damping but the best damping ratio is achieved at the load bus. Further studies were conducted considering a Type-1 exciter in the MVAC and MVDC architectures, instead of the Type-0 exciter and without considering SVC.

6.4 IEEE Type-1 Exciter

The block diagram representing the IEEE Type-1 exciter is shown in figure 6.3. The output voltage of the filter and the stabilizer output are subtracted from the reference voltage to produce the error signal. This error voltage is amplified with the help of the regulator. The limits for the regulator with time constant, T_a , and gain, K_a , depend on the amplifier power supply limitations. The output of the regulator, V_r , is subtracted from the feedback signal of the field voltage and is fed to the exciter. The excitation system stabilization is provided with the help of a signal derived from the field voltage through a feedback having a time constant T_f and gain K_f .

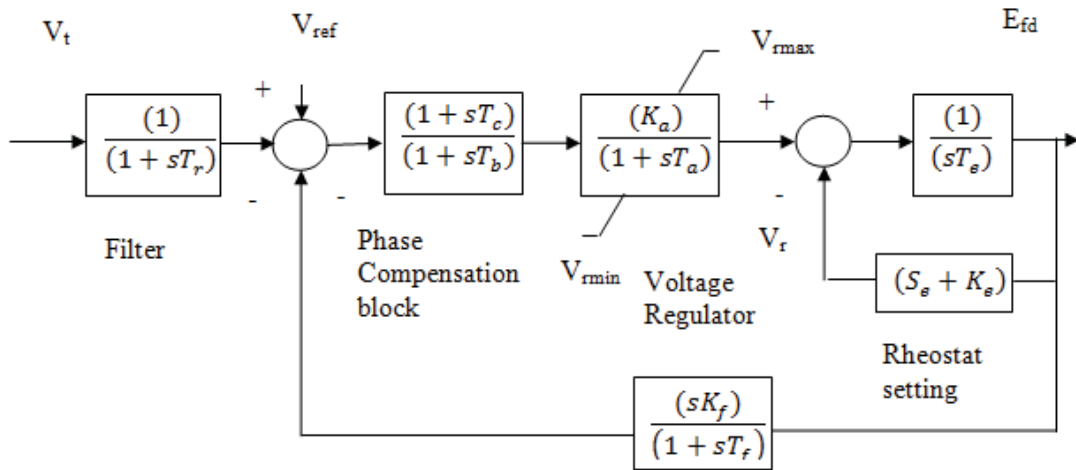


Figure 6.3 IEEE Type-1 exciter [42].

where,

T_r is the input filter time constant.

T_a , T_b and T_c are the voltage regulator time constants.

V_{rmax} and V_{rmin} are the maximum and minimum values of regulator output.

T_e is the exciter time constant.

K_a is the regulator gain.

K_e is the value of field rheostat setting.

K_f is the stabilizer gain.

T_f is the stabilizer time constant.

The plots of the eigenvalues, obtained with the Type-1 exciter for MVAC and MVDC architectures are shown in figures 6.4 and 6.5, respectively.

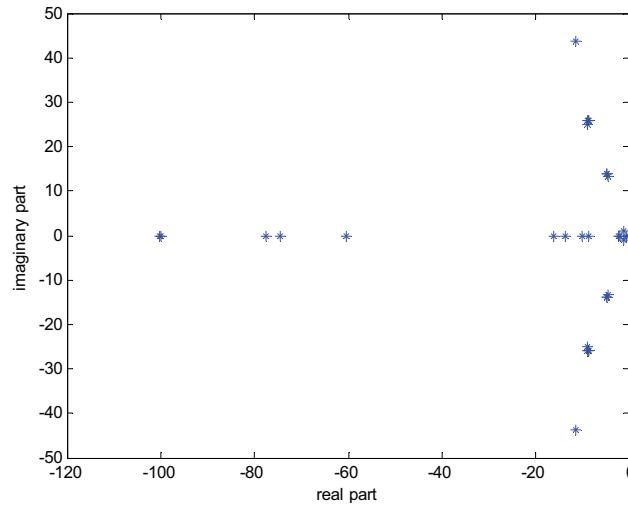


Figure 6.4 Eigenvalues for MVAC architecture with Type-1 exciter.

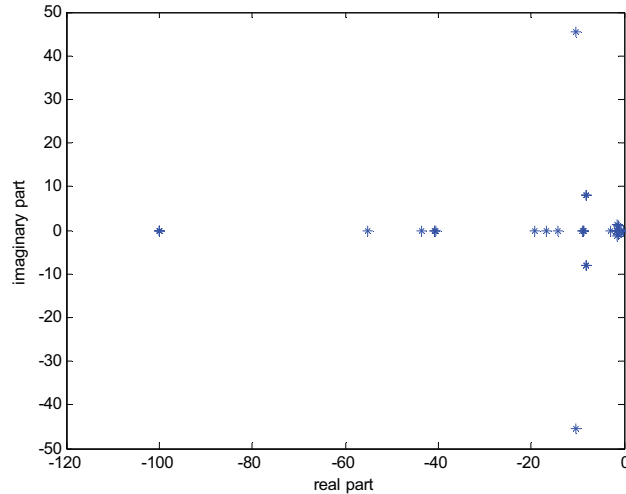


Figure 6.5 Eigenvalues for MVDC architecture with Type-1 exciter.

For the MVAC architecture with Type-1 exciter, all the eigenvalues are on the left of the complex plane exhibiting small signal stability and the damping ratio corresponding to the critical mode is found to be 0.152. Thus, use of higher order exciter control improved the damping of the system from -0.016 to 0.152. Results with the Type-1 exciter were also obtained for the MVDC architecture and it is observed that the damping ratio improves from 0.069 to 0.2228. Table 6.1 gives a summary of the eigenvalues with the SVC and with the Type-1 exciter for MVAC and MVDC architectures. It is also observed that the gain of the exciter also contributes significantly to the damping of the system.

6.5 Power System Stabilizer

The Power System Stabilizer [33] has been popularly used in terrestrial systems to improve angular stability of the system. It adds damping to the generator rotor

oscillations through the control of its excitation using stabilizing signals. The block diagram of PSS used in this part of the work is represented in figure 6.6.

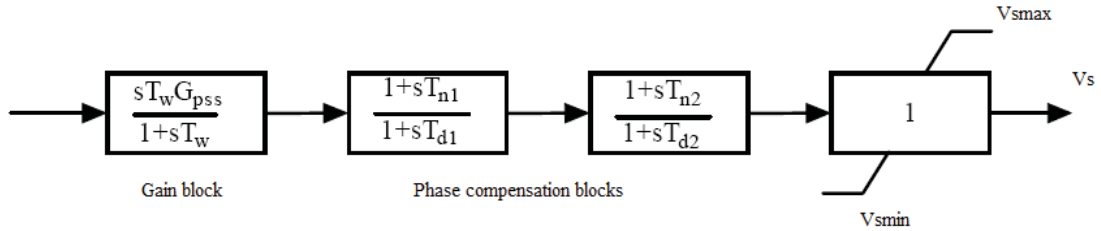


Figure 6.6 Block diagram of Power System Stabilizer [38].

where,

G_{pss} is the gain of the stabilizer.

T_w is the washout time constant.

T_{n1} and T_{n2} are the lead time constants.

T_{d1} and T_{d2} are the lag time constants.

V_{smax} and V_{smin} are the maximum and minimum limits of the output.

V_s is the stabilizer output voltage.

PSS also introduces a damping torque component to control the generator excitation. In order to examine the validity of the participation analysis in the given system architectures, which has found that the controllers, affecting voltage states and the rotor angle/speed states, will be more effective in improving the small signal stability, impact of using PSS, which derives speed deviation as the feedback signal, was studied. The stabilizing signal V_s , output of PSS block will be used to control the excitation of the generator. It does so by adding an input signal to the regulator to damp power system

oscillations and enhances small signal stability. The plot of eigenvalues for the MVAC architecture with the PSS added is shown in figure 6.7.

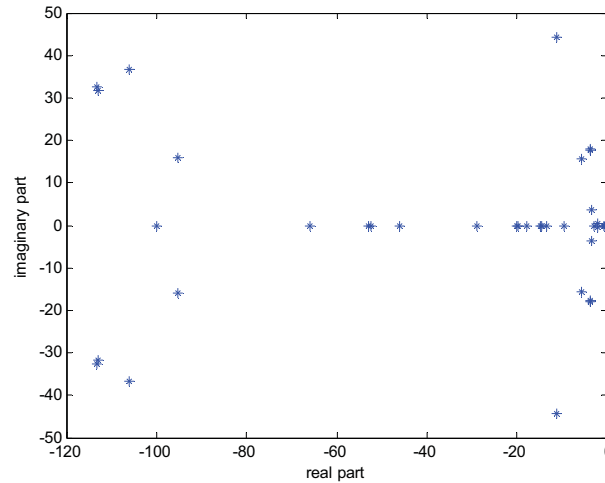


Figure 6.7 Eigenvalues for MVAC architecture with PSS.

The numbers of states (blue dots) in figure 6.7 are also more compared to the other figures. This is due to the addition of PSS which contributes to additional states. The system remains stable with all the eigenvalues lying in the left half of the complex plane. The damping ratio with the addition of PSS was 0.2022 and the damping ratio with SVC at the load bus was 0.2529. From this, it can be understood that the voltage states are significantly contributing to the damping of the system, which is in agreement with the results of participation results. A few Eigenvalues and damping ratios with Type-1 exciter for MVAC as well as MVDC architectures were also presented in table 6.2.

Table 6.2 Few critical Eigenvalues

MVAC system with 20 MVAR SVC at load bus		MVAC system with Type-1 exciter		MVDC system with Type-1 exciter		MVAC system with PSS	
Eigenvalue	Damping ratio	Eigenvalue	Damping ratio	Eigenvalue	Damping ratio	Eigenvalue	Damping ratio
-11.445 ±45.779i	0.2529	0.00 ±0.0001i	0.152	-10.564 ±45.54i	0.2228	-20± 17.876i	0.2022
-4.724 ±15.821i	0.5254	-0.114 ±0.457i	0.2552	-8.022 ±8.05i	0.7059	-19.690 ±17.815	0.2076
-4.716 ±15.655i	0.5269	-0.044 ±0.154i	0.5176	-8.062 ±8.08i	0.7061	-11.080 ±44.156	0.2434
-4.925 ±15.854i	0.5555	-0.088 ±0.257i	0.5248	-8.155 ±8.08i	0.7095	-14.816 ±15.500	0.3399
-5.657 ±5.172i	0.7556	-0.088 ±0.257i	0.5250	-1.585 ±1.185i	0.7600	-3.589 ±3.721	0.6892

6.6 Summary

This chapter has presented the results of improvement in small signal stability of MVAC and MVDC architectures of the zonal shipboard power systems through selection of proper control action. Participation analysis has been carried out in the MVAC system to identify the states participating maximum in the critical mode. A brief description of models used for the IEEE Type-1 exciter, SVC, PSS and the results obtained on both the MVAC and MVDC systems showing their impact on the improvement of damping ratio are presented.

CHAPTER 7

CONCLUSIONS AND FUTURE WORK

7.1 Conclusions

This research project has focused mainly on the rotor angle stability, i.e. transient and small signal stability of the MVDC shipboard power system. The MVDC architecture has been recently proposed for US naval shipboards and stability studies are important to establish its feasibility. Significant work has been done on terrestrial power systems to develop IGBT based DC transmission (i.e. VSC-HVDC) as given in chapter II, whereas extensive studies are required to be carried out on the shipboard power system, which will require Medium Voltage DC distribution in the range of ± 3000 V to 10000 V. This work started with the design of phase reactors, transformers, converters and capacitors to achieve a target DC voltage of 5000 V. The DC voltage control scheme [10, 35] has been implemented. The control scheme for power regulator has been implemented from [36]. A two-terminal VSC-MVDC system was first implemented to achieve the proposed shipboard power system voltage and power levels. In this system one converter controls the DC voltage across the DC bus and the other converter controls the real and reactive power. This has been extended to a MTDC ring structure, representing the notional MVDC shipboard power system. This work has focused more on the implementation of VSC-MVDC system. The following conclusions can be made on the VSC-MVDC system and MTDC ring structure.

- i) The desired voltage level of 5000 V is maintained across the DC bus by proper selection of system components in the two-terminal VSC-MVDC system.
- ii) The load voltage is maintained at 4160 V, which is the proposed voltage of AC system 2.
- iii) For the MTDC ring structure, representing the MVDC shipboard power system, a 3-phase fault at the generator terminals leads to rotor angle deviation and the system becomes unstable.

Small signal stability work has been carried out with the help of Power System Toolbox [34]. This requires representing the power system component models in mathematical form. The input file for the program requires all the parameters, describing the mathematical model given in chapter V. The program outputs the eigenvalues and damping ratios of critical modes for the given test system. Participation analysis has been utilized to identify the states participating with maximum impact on the critical mode. These were used in chapter VI to select proper controllers to improve the small signal stability. Small signal stability analysis has been carried out for the MVAC and the MVDC architectures of the shipboard power system and the following conclusions can be made.

- i) Considering the generators provided with the Type-0 exciter, the system is found to be unstable with the MVAC architecture and stable with the MVDC architecture. One pair of eigenvalues has a positive real part, and hence exhibit negative damping, in the case of the MVAC architecture.

- ii) Participation analysis reveals that the generator internal voltage state, exciter field voltage state and the propulsion motor terminal voltage state are participating significantly into the unstable mode in the MVAC architecture.
- iii) Use of a Type-1 exciter, along with a built in stabilizing and compensating circuit or with the placement of an SVC at motor terminal bus makes the MVAC system stable.
- iv) Use of Type-1 exciter in MVDC system improved the damping of the system as compared to that with the Type-0 exciter.
- v) The addition of Power System Stabilizer (PSS) improved the damping of the MVAC system with Type-0 exciter, but the damping ratio with the addition of SVC was more compared to the case with addition of PSS, which validates the results of participation analysis in the given systems.

From the above conclusions, this work has contributed the following aspects towards the stability study of shipboard power system.

- i) Selection of VSC-MVDC component values has been done to maintain 5000 VDC across the DC bus (as desired for the MVDC architecture).
- ii) The control scheme for one of the converters acting as a power dispatcher [36] has been implemented in MATLAB Simulink.
- iii) A two-terminal VSC-MVDC system was implemented in MATLAB Simulink.
- iv) This system was extended to a multi-terminal DC ring structure similar to the shipboard power system with two synchronous generators and transient stability analysis was carried out.

- v) Power System Toolbox was used to determine and demonstrate the small signal stability of MVAC and MVDC architectures of the shipboard power system.

7.2 Future Work

This work has implemented a MTDC structure similar to the shipboard power system, but using simplified architecture considering only two synchronous machines for the transient analysis. Further research work can be done considering the following aspects.

- i) The MTDC ring structure can be extended to include all the four synchronous machines (i.e. two main generators and two auxiliary generators) as envisioned in the notional shipboard power systems.
- ii) The distortion in the DC link voltages in MTDC ring structure can be attributed to the need of having better filters in the system. Improvement can be made in selection of proper filters to decrease the distortion.
- iii) DC circuit breakers can be added to implement the zonal shipboard power system.
- iv) Voltage stability and frequency stability studies can be performed on the MTDC ring structure.

The following improvements can be done in the small signal stability work.

- i) Converter dynamics can also be included while carrying out the small signal stability analysis.
- ii) Improvement in system stability may require designing supplementary controllers with the converter dynamics included in the study, which may be explored.

REFERENCES

- [1] Norbert Doerry, Next Generation Integrated Power System Technology Development Roadmap, November 2007.
- [2] P. Kundur et al., "Definition and classification of power system stability IEEE/CIGRE joint task force on stability terms and definitions," *IEEE Transactions on Power. Systems*, vol. 19, no. 3, pp. 1387-1401, Aug. 2004.
- [3] C. Petry and J. Rumburg, "Zonal Electrical Distribution Systems: An Affordable Architecture for Future," *Naval Engineers Journal*, Vol.105, pp. 45-51, May 1993.
- [4] John G. Ciezki and Robert W. Ashton, "Selection and Stability Issues Associated with a Navy Shipboard DC Zonal Electric Distribution System", *IEEE Transactions on Power Delivery*, Vol. 15, No. 2, pp. 665-669, April 2000.
- [5] RTDS Notional E-ship model Technical guide, *Florida State University*, Version 3.4, June 2008.
- [6] J. Arrillaga, High Voltage Direct Current Transmission, Peter Peregrinus Ltd., London, UK.
- [7] K. R. Padiyar, HVDC Power Transmission Systems Technology and System Interactions, John Wiley & Sons, Inc., 1990.
- [8] C. Du, A. Sannino, and M. Bollen, "Analysis of the Control Algorithms of Voltage-Source Converter HVDC", *Proceedings of IEEE- PES Power Tech 2005*, St. Petersburg, June 2005.
- [9] A Lindberg and T Larsson, "PWM and Control of Three Level Voltage Source Converters in a HVDC Back-to-Back Station", *AC and DC Power Transmission*, No. 423, pp. 297-302, April 1996.
- [10] C. Bajracharya, M. Molinas, J. A. Suul and T. M. Undeland, "Understanding of Tuning Techniques of Converter Controllers for VSC-HVDC", *Nordic Workshop on Power and Industrial Electronics*, June 2008.

- [11] Weixing Lu and Boon Teck Ooi, “Simultaneous inter-area decoupling and local area damping by voltage source HVDC”, *Proceedings of IEEE PES Winter Meeting*, Columbus, pp. 1079-1084, 2001.
- [12] Weixing Lu, “Control and Application of Multi-terminal HVDC Based on Voltage-Source Converter”, PhD dissertation, McGill University, Canada, 2003.
- [13] HVDC and HVDC Light obtained from [http:// www.abb.com/industries/us](http://www.abb.com/industries/us)
- [14] Introduction to HVDC Plus obtained form [http:// www.energy-portal.siemens.com](http://www.energy-portal.siemens.com)
- [15] HVDC Plus Technologies obtained from [http:// www.ci.pittsburg.ca.us/pit/pdf/....2-ProjDescription.htm](http://www.ci.pittsburg.ca.us/pit/pdf/....2-ProjDescription.htm)
- [16] U. Axelsson, A. Holm, C. Liljegren, K. Eriksson and L. Weimers, “ Gotland HVDC Light Transmission- World’s First Commercial Small Scale DC Transmission”, *CIGRE Conference*, France, May 1999.
- [17] K. Hobrunk, P.L. Sorensen, P. Christensen, N. Andersen, K. Ericsson and P. Holmberg, “ DC Feeder for Connection of a Wind Farm”, *CIGRE Symposium*, Kuala Lumpur, Malaysia, September 1999.
- [18] N. G.Hingorani and L. Gyugyi, Understanding FACTS, IEEE Press: New York, 2001.
- [19] Pulse Width Modulation diagram obtained from [http:// www.mathworks.com](http://www.mathworks.com)
- [20] Jose Sayago, “Three Level Neutral Point Clamped Voltage Source Converter”, *Leistungs Elektronik manual*.
- [21] Two and Three level Voltages obtained from [http:// www.mathworks.com](http://www.mathworks.com)
- [22] Povilas Zizliauskas, “Subsynchronous Torque Interaction for HVDC Light B”, MSc. Thesis, Lund University, 2001.
- [23] C. Du and M. Bollen, “ A New Contol Strategy of a VSC-HVDC System for High-Quality supply of Industrial Plants”, *IEEE Transactions on Power Delivery*, Vol.22, No.4, pp. 2389-2394, October 2007.

- [24] G. Asplund, “Application of HVDC Light to Power System Enhancement”, *IEEE Winter Power Meeting*, Singapore, January 2000.
- [25] W. Lu and B. T. Ooi, “ DC Over-Voltage Control during Loss of Converter in Multi-Terminal Voltage- Source Converter Based HVDC (M-VSC-HVDC)”, *IEEE Transactions on Power Delivery*, Vol.18, No.3, pp. 915-920, July 2003.
- [26] Weixing Lu and B. T. Ooi, “ Multiterminal LVDC System for Optimal Acquisition of Power in Wind- Farm Using Induction- Generators” , *IEEE Transactions on Power Electronics*, Vol. 17, No. 4, pp. 558- 563.July 2002.
- [27] Weixing Lu and B. T. Ooi, “ Optimal Acquisition and Aggregation of Offshore Wind- Power by Multi-Terminal Voltage- Source HVDC”, *IEEE Transactions on Power Delivery*, Vol.18, No.1, pp. 201- 206, January 2003.
- [28] L. Tang and B. T. Ooi, “Elimination of Harmonic Transfer Through Converters in VSC MTDC system by AC/DC decoupling” , *IEEE Transactions On Power Delivery*, Vol. 23, No. 1, pp. 402- 409, January 2008.
- [29] G. Reed, R. Pape and M. Takeda, “ Advantages of Voltage-Sourced Converter (VSC) Based Design Concepts for FACTS and HVDC-Link Applications”, *IEEE Power Engineering Society General Meeting*, Vol.3, pp. 1816-1821, July 2003.
- [30] C. Du and E. Agneholm, “A Novel Control of VSC-HVDC for Improving Power Quality of an Industrial Plant”, *Proceeding of 32nd Annual conference on IEEE Industrial Electronics*, pp. 1962-1967, November 2006.
- [31] C. Du, E.Agneholm and G. Olsson, “Use of VSC-HVDC for Industrial Systems having Onsite Generation with Frequency Control”, *IEEE Transactions on Power Delivery*, Vol. 23, No. 4, pp. 2233-2240, Oct 2008.
- [32] G. J.Li, T. T.Lie, Y. Z. Sun, L. Peng and X. Li “ Applications of VSC- Based HVDC in Power System Stability Enhancement”, *Power Engineering Conference*, 2005.
- [33] Prabha Kundur, Power System Stability and Control, New York: McGraw-Hill Inc, 1994.
- [34] Power System Toolbox, Cherry Tree Scientific software, Version 3, Canada. Obtained form [http:// www.eagle.ca/~cherry/pst3.htm](http://www.eagle.ca/~cherry/pst3.htm)
- [35] Three level VSC Rectifier demo obtained from [http:// www.mathworks.com/demos/](http://www.mathworks.com/demos/)

- [36] Y. Ming, Li Gengyin, L. Guangkai, L. Haifeng and Z. Ming, “ Modeling of VSC-HVDC and Its Active Power Control Scheme”, *International Conference on Power System Technology*, pp. 1351-1355, November 2004.
- [37] A.J.J. Rezek, C. A. D. Coelho, J. M. E. Vincente, A. Cortez and P. R. Laurentino, “ The Modulus Optimum (MO) Method Applied to Voltage Regulation Systems: Modeling, Tuning and Implementation”, *Proceedings International Conference on Power System Transients*, Brazil, June 2001.
- [38] Graham Rogers, Power System Oscillations, Kluwer Academic Publishers, 2000.
- [39] Yao-Nan Yu, Electric Power system Dynamics, New York: Academic Press, 1983.
- [40] Peter W. Sauer and M. A. Pai, Power System Dynamics and Stability, New Jersey: Prentice Hall, 1998.
- [41] Marija Ilic and John Zaborszky, Dynamics and Control of Large Electric Power Systems, New York: Wiley- Interscience, 2000.
- [42] IEEE Committee Report, "Excitation System Models for Power System Stability Studies," *IEEE Transactions of Power Apparatus and Systems*, Vol. PAS-100, pp. 494-509, 1981.
- [43] S. Ahmed- Zaid and M. Taleb, “Structural Modeling of Small and Large Induction Machines Using Integral Manifolds”, *IEEE Transactions on Energy Conversion*, Vol. 6, No. 3, pp. 529- 535, Sep 1991.
- [44] Xiao-Ping Zhang, “Multi Terminal Voltage- Sourced Converter-Based HVDC models for Power Flow Analysis”, *IEEE Transactions on Power Systems*, Vol 19, No.4, pp. 1877-1883, Nov 2004.
- [45] E. V. Larsen and J. H. Chow, "SVC Control Concepts for System Dynamic Performance," *Application of Static Var Systems for System Dynamic Performance*, IEEE Publications 87TH0187-5-PWR, 1987.
- [46] Thomas L. Baldwin and Shani A. Lewis, “Distribution Load Flow Methods for Shipboard Power Systems”, *IEEE Transactions on Industry applications*, Vol. 40, No.5, pp. 1183-1190, Sep/Oct 2004.

- [47] Ned Mohan, Tore M. Undeland and William P. Robbins, Power Electronics-Coverters, Applications and Design, John Wiley & Sons, 1995.
- [48] Norman S. Nise, Control Systems Engineering, The Benjamin/Cummings Publishing Company Inc., 1992.
- [49] “Gexol World Class Marine Cables” by Americable Incorporated obtained from <http://www.1st4cables.com/downloads/gexolcatalog.pdf>
- [50] Seetharama R Rudraraju, Anurag K Srivastava, Suresh C Srivastava and Noel N Schulz, “Small Signal Stability Analysis of a Shipboard MVDC Power System”, IEEE Electric Ship Technologies Symposium (ESTS) Conference, Baltimore, MD, April 2009.